Journal of Integrative Agriculture 2026, 25(3): 847–863

KeAi
CHINESE ROOTS
GLOBAL IMPACT

Available online at ScienceDirect

Journal of Integrative Agriculture



RESEARCH ARTICLE

Genome-wide association study reveals genomic regions for nitrogen, phosphorus and potassium use efficiency in bread wheat

Jili Xu[1*], Shuo Liu[2*], Zhiyuan Gao[1*], Qingdong Zeng[3], Xiaowen Zhang[1], Dejun Han[4#], Hui Tian[1#]

[1] *College of Natural Resources and Environment, Northwest A&F University/Key Laboratory of Plant Nutrition and the Agri-environment in Northwest China, Ministry of Agriculture and Rural Affairs, Yangling 712100, China*
[2] *Cultivated Land Quality Protection Station, Lianyungang Agricultural and Rural Bureau, Lianyungang 712100, China*
[3] *State Key Laboratory of Crop Stress Resistance and High-Efficiency Production/College of Plant Protection, Northwest A&F University, Yangling 712100, China*
[4] *State Key Laboratory of Crop Stress Resistance and High-Efficiency Production/College of Agronomy, Northwest A&F University, Yangling 712100, China*

Highlights

- A total of 534 quantitative trait loci (QTLs) were identified though genome-wide association study (GWAS).
- Through integrated meta-QTL analysis, QTL80, QTL387, and QTL500 were found to be co-localized quantitative trait loci, while QTL234 was identified as a novel locus.
- A dCAPS marker was developed for the SNP (*AX-109095537*) within the nitrogen harvest index (NHI)-associated QTL234.

Abstract

The development of wheat cultivars with improved nitrogen (N), phosphorus (P), and potassium (K) use efficiency is essential for sustainable agriculture. Genetic dissection and identification of causative genes underlying nutrient use efficiency represent a key strategy toward this goal. We conducted an extensive genome-wide association study (GWAS) using a panel of 431 wheat cultivars, identifying 1,659 significant single-nucleotide polymorphisms (SNPs) (LOD>5) through genotyping-by-sequencing. This analysis revealed 534 quantitative trait loci (QTLs) associated with 12 nutrient use efficiency traits across five distinct environments, among which 14 QTLs were consistently detected in at least three environments. Notably, meta-QTL analysis, showed that QTL80 (72.12–74.24 Mb, chr2A), QTL387 (32.88–33.56 Mb, chr6A), and QTL500 (535.53–540.80 Mb, chr7B) exhibit clear co-localization with MQTL-2A-2, MQTL-6A-1, and MQTL-7B-2, respectively. This overlap highlights their robustness across diverse environmental conditions. Within these regions, critical candidate genes — including members of the bZIP transcription factor family and a potassium transporter gene — were identified in relation to nutrient use efficiency. Furthermore, a novel locus, QTL234, was discovered, harboring key candidate genes such as dof zinc finger protein, Ankyrin repeat family protein, and cytochrome P450. To validate the SNP within QTL234 associated with nitrogen harvest index (NHI), we developed a dCAPS marker for *AX-109095537*. These findings demonstrate the effectiveness of high-resolution SNP-based GWAS in rapidly pinpointing promising candidate genes. They also establish a foundation for large-scale QTL fine mapping, candidate gene validation, and the development of functional markers essential for enhancing nutrient use efficiency in wheat breeding programs.

Keywords: wheat, genome-wide association study, nutrient use efficiency, meta-QTL analysis, candidate genes

Received 24 February 2024; Received in revised form 25 April 2024; Accepted 6 May 2024; Available online 27 June 2024
Jili Xu, E-mail: 2021060380@nwafu.edu.cn; Shuo Liu, E-mail: 732361104@qq.com; Zhiyuan Gao, E-mail: 739162009@qq.com; [#]Correspondence Dejun Han, E-mail: handj@nwsuaf.edu.cn; Hui Tian, E-mail: tianh@nwsuaf.edu.cn
[*] These authors contributed equally to this study.

© 2026 CAAS. Publishing services by Elsevier B.V. on behalf of KeAi Communications Co. Ltd. This is an open access article under the CC BY-NC-ND license (http://creativecommons.org/licenses/by-nc-nd/4.0/). Peer review under responsibility of Editorial Board of *Journal of Integrative Agriculture*.
doi: 10.1016/j.jia.2024.06.012

1. Introduction

The first Green Revolution, beginning in the mid-20th century, led to a substantial increase in global wheat grain production through the adoption of high-yielding cultivars, chemical fertilizers, and synthetic pesticides. However, low nutrient use efficiency has emerged as a critical constraint to sustainable wheat production worldwide. In Chinese wheat systems, the in-season nitrogen (N) recovery efficiency (RE_N) of applied N fertilizer is less than 40% (Giordano *et al*. 2023), while nitrogen use efficiency (NUE) has also declined across Europe, Asia, and America over recent decades (Leip *et al*. 2018). Phosphorus use efficiency (PUE) is even lower, with in-season recovery rates ranging from 10 to 20% (Kreutz *et al.* 2022), primarily due to the rapid immobilization of soluble phosphate into insoluble forms in soil. Although potassium (K) fertilizer exhibits higher utilization efficiency compared to N and P (Rengel and Damon 2008), enhancing potassium use efficiency (KUE) remains essential given the rising cost of K fertilizers and finite potash reserves. Low nutrient use efficiency not only increases wheat production costs but also exacerbates environmental problems such as water eutrophication (Yang *et al*. 2024), greenhouse gas emissions (Kusin *et al*. 2015), and soil acidification (Hao *et al*. 2020). Currently, wheat breeding programs primarily target traits such as dwarfism, resistance to biotic and abiotic stresses, and grain quality, largely independent of nutrient input levels. Nevertheless, nutrient use efficiency must be recognized as a key breeding objective in future efforts to achieve sustainable productivity.

Genetic variation in NUE, PUE, and KUE among wheat genotypes has been well documented (Patial 2021). These traits exhibit quantitative inheritance and are governed by multiple genes or quantitative trait loci (QTLs). Over the past two decades, several key QTLs associated with NUE, PUE, and KUE have been identified in wheat (Yang M J *et al.* 2021). For example, six QTLs related to NUE were detected in winter wheat across multiple environments using genetic linkage maps (Brasier *et al*. 2020). Similarly, seven QTLs influencing P uptake efficiency and six affecting P utilization efficiency were identified using a double haploid (DH) population derived from two Chinese winter wheat varieties (Su *et al*. 2009). However, QTLs identified in biparental populations are strongly influenced by genetic background and environmental conditions, which limits their stability and broad applicability in breeding programs (Thiemann *et al*. 2014). Meta-analysis of QTLs enables the identification of consensus and stable genomic regions by integrating results from independent studies, regardless of population type, genetic background, location, or year. This approach has been successfully applied in wheat for various traits, including yield and its components (Zhang *et al*. 2010), NUE-related traits (Quraishi *et al*. 2011), and root architecture (Darzi-Ramandi *et al*. 2017; Saini *et al*. 2021). Quraishi *et al*. (2011) identified meta-QTLs (MQTLs) on chromosomes 2A, 2B, 4B, and 5A associated with NUE components, which co-localize with homologs of the *Ppd-A1* and *Ppd-B1* genes (Arjona *et al*. 2018), photoperiod sensitivity loci, and dwarfing genes *Rht-B1* and *Rht*-D1 (Peng *et al*. 1999), respectively. Saini *et al*. (2021) conducted a meta-QTL analysis for NUE and root system architecture in bread wheat, identifying 93 candidate genes, including those encoding Cytochrome P450, GRAS transcription factors, RING-type zinc finger proteins. Despite these advances, comprehensive meta-analyses of QTLs governing NUE, PUE, and KUE in wheat remain lacking.

Recent advancements in next-generation sequencing (NGS) technologies have made genome-wide association studies (GWAS) a powerful tool for detecting associations between phenotypic variation and single-nucleotide polymorphisms (SNPs) (Yan *et al.* 2023; Zhang *et al.* 2023). GWAS offers enhanced marker resolution and facilitates the dissection of complex trait architectures in diverse germplasm panels (Ober *et al.* 2010; Ma *et al.* 2018). Safdar *et al*. (2021) performed a GWAS on P utilization efficiency using the wheat 90K SNP array and identified the candidate gene *TraesCS4A02G481800*, which participates in pyruvate metabolism and the tricarboxylic acid (TCA) cycle and shows significantly higher expression in P-efficient genotypes under low-P conditions. Another study employing the 35K Wheat Breeder's Affymetrix array identified 297 genes associated with carbohydrate metabolism, fatty acid biosynthesis, protein phosphorylation/dephosphorylation, transmembrane transport, and nucleotide biosynthesis under low-phosphorus conditions (Soumya *et al*. 2021). Additionally, Safdar *et al*. (2020) identified 20 putative candidate genes involved in stress tolerance, sugar metabolism, and nutrient transport that influence KUE and agronomic performance in bread wheat using the 90K Infinium SNP array. Sun *et al*. (2020) reported that the wheat 35K (97.44%) and 90K (86.9%) SNP arrays contain a lower proportion of genome-specific SNPs compared to the 660K array (99.05%), which provides more reliable physical positions. However, low-density SNP arrays are generally insufficient to capture sufficient genome-wide association signals for accurate QTL and candidate gene mapping. Moreover, due to the complexity and polyploidy of the wheat genome, the genetic basis of N, P, and K use efficiencies remains incompletely characterized.

In this study, we genotyped a large panel of 431 wheat cultivars — representing diverse release years, geographical origins, life habitats, and plant heights — using the 660K SNP array. We then conducted a GWAS on 12 key N, P, and K use efficiency traits, leveraging multi-environment phenotypic data collected across China. The primary objectives were to (1) evaluate the genetic and phenotypic diversity within the cultivar panel; (2) dissect the genetic architecture of nutrient use efficiency traits and identify associated QTLs through GWAS; and (3) perform a meta-analysis of previously published QTLs related to nutrient use efficiency in wheat. This integrative analysis aimed to consolidate GWAS findings, reveal co-localized QTL regions, and pinpoint candidate genes underlying nutrient use efficiency.

2. Materials and methods

2.1. Plant materials and growth conditions

The plant materials consisted of 431 wheat cultivars obtained from the wheat germplasm bank at Northwest A&F University,

China. Of these, 364 were collected from major wheat-producing regions across China, while the remaining 67 originated globally (Appendix A). All cultivars were grown across five environments: the Experiment Station of Yangling (34.28°N, 108.07°E, 521 m a.s.l.) in Shaanxi Province during the 2018–2019 growing season (19YL); Nanyang (32.98°N, 112.53°E, 131 m a.s.l.) in Henan Province during 2018–2019 (19NY) and 2019–2020 (20NY); Luoyang (34.62°N, 112.45°E, 144 m a.s.l.) in Henan Province during 2019–2020 (20LY); and Suqian (33.86°N, 118.27°E, 23 m a.s.l.) in Jiangsu Province during 2019–2020 (20SQ). Prior to sowing, soil physicochemical properties — including pH (soil:water ratio=1:2.5), organic matter, NH_4^+, NO_3^-, available P, and available K — were analyzed at all five sites. The NO_3^--N content was 26.7, 35.6, 41.4, 8.45, and 13.3 mg kg^{-1}; NH_4^+-N content was 0.39, 1.53, 5.12, 3.80, and 1.37 mg kg^{-1}; available P was 9.20, 21.8, 26.1, 6.60, and 7.71 mg P_2O_5 kg^{-1}; available K was 145.5, 125.5, 92.2, 238.6, and 147.8 mg K_2O kg^{-1}; organic matter was 13.0, 18.6, 17.3, 24.8, and 22.0 g kg^{-1}; and pH values were 8.06, 5.74, 5.21, 8.02, and 8.25 in 19YL, 19NY, 20NY, 20LY, and 20SQ, respectively. An augmented complete block design was employed, with fourteen blocks (6 m×35 m), each containing five control wheat cultivars (Zhoumai 18, Yanzhan 4110, Xinong 511, Jimai 22, and Bainong 207). The experiment comprised 14 blocks: blocks 1 to 13 each included 36 wheat cultivars (including the five controls), while block 14 contained 34 cultivars. Each accession was space-planted in a single row measuring 3 m in length, with six rows per plot, 2.5 cm between plants, and 20 cm between rows. Nitrogen application rates were 172, 170, 192, 164, and 251 kg N ha^{-1}; phosphorus rates were 112, 101, 124, 113, and 113 kg P_2O_5 ha^{-1}; and potassium rates were 0, 101, 124, 113, and 113 kg K_2O ha^{-1} at 19YL, 19NY, 20NY, 20LY, and 20SQ, respectively. Detailed information on soil conditions and fertilizer application rates is provided in Xu *et al.* (2022). Throughout each growing season, field management followed standard local wheat production practices.

2.2. Phenotyping details

At maturity, the central row (3 m-long) of each plot was harvested to measure grain yield in oven-dried weight. To determine N, P, and K concentrations, 30 tillers were randomly collected from each plot, and ears were separated into grains and glumes. Grain, shoot, and glume samples were oven-dried at 65°C, and the grain/shoot and grain/glume ratios were calculated. Shoot biomass (dry weight, kg ha^{-1}) and glume biomass (dry weight, kg ha^{-1}) were computed as follows:

Shoot biomass (in dry weight, kg ha^{-1})=Grain yield (kg ha^{-1})/(Grain/Shoot)

Glume biomass (in dry weight, kg ha^{-1})=Grain yield (kg ha^{-1})/(Grain/Glume)

The oven-dried samples were ground using a ball mill (MM400, RETSCH, Germany) equipped with tungsten carbide jars and stored in sealed polyethylene bags prior to chemical analysis. Plant material was digested with H_2O_2-H_2SO_4 for determination of total N, P, and K concentrations. Concentrations of N and P in the digestate were quantified using a high-resolution digital colorimeter Auto Analyzer 3 (AA3, SEAL Co., Germany). Potassium concentration was determined *via* flame spectrophotometry (Model 410, Sherwood Co., England).

2.3. Phenotypic analysis of N, P and K use efficiency parameters

Total aboveground N content (TN) was calculated as follows:

TN (kg N ha^{-1})=(GNC×GY)+(SNC×SY)+(GLNC×GLY)

where GNC is the grain N concentration (%), GY is the grain yield (kg ha^{-1}), SNC is the straw N concentration (%), SY is the straw yield (kg ha^{-1}), GLNC is the glume N concentration (%), and GLY is the glume yield (kg ha^{-1}).

NUE comprises nitrogen uptake efficiency and nitrogen utilization efficiency. Specifically, N utilization efficiency based on grain yield (GNUE), N utilization efficiency based on total aboveground biomass yield (SNUE), N uptake efficiency (NUPE), and N harvest index (NHI) were calculated as follows:

$$\text{GNUE (kg grain kg}^{-1}\text{ N)}=\frac{\text{GY}}{\text{TN}}$$

$$\text{SNUE (kg aboveground dry matter kg}^{-1}\text{ N)}=\frac{\text{TSB}}{\text{TN}}$$

$$\text{NUPE (kg N uptake at harvest kg}^{-1}\text{ available N from soil and fertilizer)}=\frac{\text{TN}}{N_{ava}+N_{fer}}$$

$$\text{NHI}=\frac{\text{GNC}\times\text{GY}}{\text{TN}}$$

where TSB is total aboveground dry matter biomass, calculated as TSB=GY+SY+GLY; N_{ava} is soil-available N (kg N ha^{-1}); and N_{fer} is N applied *via* fertilizer (kg N ha^{-1}).

P and K use efficiency parameters were computed using the same method as their nitrogen-based counterparts. These parameters for P use efficiency included P utilization efficiency based on grain yield (GPUE), P utilization efficiency based on total aboveground biomass yield (SPUE), P uptake efficiency (PUPE), and P harvest index (PHI). Similarly, K use efficiency parameters included K utilization efficiency based on grain yield (GKUE), K utilization efficiency based on total aboveground biomass yield (SKUE), K uptake efficiency (KUPE), and K harvest index (KHI).

2.4. Genotypic analysis

The association panel, comprising 437 accessions, was genotyped using the wheat 660 K Illumina Infinium SNP array. SNP genotype calling and allele clustering were performed using the polyploid version of Affymetrix Genotyping ConsoleTM (GTC) software. The data were filtered to exclude SNPs with a call rate below 0.9 (i.e., detection failure rate exceeding 0.1), a minor allele frequency less than 0.05, or a Hardy-Weinberg Equilibrium (HWE) *P*-value greater than 0.01. To determine the physical positions of SNPs, probe sequences were aligned to the IWGSC RefSeq v1.0 reference genome using Nucleotide-Nucleotide BLAST (BLASTN) software (version 2.2.29+). The polymorphism information content (PIC) value was calculated using the formula PIC=1–$\sum P_i^2$, where P_i represents the frequency of the *j*th allele at the *i*th locus.

2.5. Genome-wide linkage disequilibrium and population structure analysis

Genome-wide linkage disequilibrium (LD) analysis for the A, B, and D genomes was conducted on 437 accessions using PLINK software. LD calculation and decay analysis were performed across the entire wheat genome and for each of the individual A, B, and D sub-genomes following the methodology described by Yu *et al*. (2020). A critical significance threshold for r^2 was defined as 0.1, and the physical distance at which the LD curve intersected this threshold was taken as the average LD decay distance. LD block size was estimated as the physical distance spanned by two or more SNPs exhibiting $r^2 \geq 0.5$, measured between the outermost flanking SNPs. Population structure (Q matrix) was analyzed using STRUCTURE 2.3.4 software, with the putative number of subpopulations (K) tested from 1 to 12, each replicated five times independently. The burn-in period was set to 10,000 iterations, followed by 100,000 Markov Chain Monte Carlo (MCMC) replications after burn-in. Following Earl and Vonholdt (2012), the optimal K value was determined based on the highest Δ*K* value. Kinship (K matrix) and pedigree analyses were conducted using TASSEL 5.0 software.

2.6. Genome-wide association analysis (GWAS)

GWAS were conducted using a univariate linear mixed model implemented in GEMMA software (Zhou and Stephens 2012). The Q+K model, which incorporates population structure and kinship matrix as covariates, was applied to reduce false-positive associations. The suggestive significance threshold for *P*-values (*P*=1/Ne) was determined using a modified Bonferroni correction, where Ne represents the effective number of independent SNPs, as described by Li *et al*. (2012). A *P*-value threshold of 1.0×10^{-5} was set to define genome-wide significant SNPs. GWAS results were visualized using a Manhattan plot, and the distribution of observed *P*-values was evaluated *via* a quantile-quantile (Q-Q) plot, both generated with the QQman package in R 3.0.3. The phenotypic variance explained by significant SNPs (R^2) was estimated using GCTA software.

2.7. Meta-QTL analysis

A comprehensive review of recently published quantitative trait locus (QTL) mapping studies for NUE, PUE, and KUE in both bread and durum wheat, spanning the years 2000 to 2020, was conducted. A total of 15 studies, encompassing both pot and field experiments, were selected for meta-QTL analysis (Appendix B). Essential data from these studies are summarized in Appendix B. The QTLs directly associated with NUE, PUE, and KUE traits are listed in Appendix C, with detailed information systematically compiled for each reported QTL, including: (1) associated traits; (2) type of QTL mapping population (F_2, DH, RIL, and backcross); (3) population size; (4) LOD value; (5) R^2 or phenotypic variation explained (PVE); and (6) flanking or closely linked markers. For studies lacking reported LOD and R^2 values, default thresholds of 3 and 10%, respectively, were applied based on established precedent (Venske *et al*. 2019). The selected QTLs, annotated with key parameters such as PVE, LOD scores, peak positions, and confidence intervals (CI), were projected onto integrated genetic maps following established protocols (Cui *et al*. 2014). When original CIs were unavailable, 95% CIs were estimated using population-specific equations derived by Darvasi and Soller (1997) and Guo *et al*. (2006). Using BioMercator V4.2.3 software, independent genetic maps were integrated into a consensus framework, enabling recalibration of marker and QTL positions. Subsequently, meta-QTL analysis was performed in BioMercator V4.2.3, adhering to standardized procedures outlined by Arcade *et al*. (2004), Veyrieras *et al*. (2007), and Sosnowski *et al*. (2012). All identified meta-QTLs (MQTLs) were aligned to the wheat reference genome and systematically compared with significantly associated loci detected in the GWAS.

2.8. *In silico* prediction of candidate genes

High-confidence annotated genes within the physical intervals of the identified QTLs were retrieved from the IWGSC reference genome v1.1 (Eversole 2013). Expression data for these candidate genes were obtained from expVIP (http://www.wheat-expression.com/), a publicly available wheat expression platform.

2.9. (d)CAPS maker on the significant SNP

The significant SNP with a high LOD score within the key QTL interval was selected for conversion into a dCAPS marker. In this study, the C/T polymorphism within *TraesCS3B02G904700LC.1*, located at position 828,672,555 bp on chromosome 3B, was converted into a functional dCAPS marker designated dCAPS-555. The design of the dCAPS primers and selection of the restriction enzyme were performed using dCAPS Finder2.0 (http://helix.wustl.edu/dcaps/dcaps.html) (Neff *et al*. 2002). A G-to-T mutation was introduced at the second nucleotide downstream of the SNP to generate the *Bsm*AI recognition sequence 5′-GTCTCN-3′, thereby creating a cleavage site. However, because one of the resulting restriction fragments would have been too short for reliable detection, the 5′ end of the forward primer was extended using fusion PCR. Using genomic DNA as a template, two overlapping fragments were amplified separately using the following primers: SNP555-1F (CAAACCCAAAGGCCACAATGCTGC) and SNP555-1R (GACGGCCGAGTACTTGCCATCCGCAGTCCACCTCCATCGCATGCCGTCC), SNP555-2F (GGCATGCGATGGAGGTGGACTGCGGATGGCAAGTACTCGGCCGTC), and SNP555-2R (AAGGGCCTGCCCAGAGTGTTCGCCG).

3. Results

3.1. Population structure and linkage disequilibrium analysis

Before conducting GWAS, the 660 K SNP genotyping assay was subjected to filtering in TASSEL software. Ultimately, 412,224 SNPs were retained for further analysis, meeting the criteria of a minor allele frequency (MAF)≥0.05 and missing data≤10%.

The mean r^2 values for the A, B, and D sub-genomes, as well as the entire genome, gradually decreased with

increasing pairwise distance (Fig. 1-A). LD was calculated using 77,787, 77,778, 10,291, and 1,996 post-filtered SNP markers from the A, B, and D sub-genomes, respectively. The LD decay patterns varied by sub-genome and across chromosomes. In the D sub-genome, LD declined rapidly at first, followed by a plateau. The LD decay distance, defined as the physical distance at which r^2 dropped to 0.1, was 1.6 Mb in the D sub-genome, compared to 3.0 and 5.9 Mb in the A and B sub-genomes, respectively. The overall genome-wide LD decay occurred at 3.7 Mb.

The optimal number of sub-populations (K) was determined by plotting Δ*K* values, calculated using STRUCTURE software based on the filtered markers. Δ*K* peaked at K=7, indicating the presence of seven distinct sub-groups — designated Sub-1, Sub-2, Sub-3, Sub-4, Sub-5, Sub-6, and Sub-7 — comprising 70, 47, 46, 75, 70, 48, and 75 accessions, respectively (Fig. 1-B). Sub-1 primarily included wheat cultivars grown in North China. Sub-2 mainly consisted of semi-dwarf and tall Chinese landraces released before 1950. Sub-3 predominantly included semi-dwarf or tall Chinese landraces and cultivars released prior to 2000. Sub-4 mainly comprised wheat cultivars cultivated in North China. Sub-5 and Sub-7 primarily contained semi-dwarf or tall wheat cultivars with diverse geographic origins. Sub-6 mainly consisted of spring-type, semi-dwarf or tall Chinese landraces (Appendix A).

3.2. Phenotypic data analysis

Four out of twelve parameters appeared to follow a normal distribution, and all exhibited notable variation among cultivars (Fig. 2). The ranges of NHI, PHI, and KHI were 0.12–0.97, 0.34–1.0, and 0.01–0.67, respectively. NUPE, PUPE, and KUPE ranged from 0.04 to 0.98 kg kg^{-1}, 0.02 to 0.57 kg kg^{-1}, and 0.02 to 1.58 kg kg^{-1}, respectively. GNUE, GPUE, and GKUE varied from 7.73 to 116.7 kg kg^{-1}, 77.0 to 391.2 kg kg^{-1}, and 5.13 to 122.1 kg kg^{-1}, respectively. SNUE, SPUE, and SKUE ranged from 24.22 to 178.3, 319.1 to 1,501.6, and 35.60 to 238.4 kg kg^{-1}, respectively. Strong positive correlations were observed between GNUE and NHI, PHI and NHI, NUPE and PUPE, KHI and GKUE, and GKUE and SKUE (|*r*|>0.8). Weak but significant positive correlations included those between GNUE and GPUE, and SNUE and GPUE. Additionally, significant negative correlations were observed, such as between NUPE and GNUE, and between KHI and KUPE, though all were weak (|*r*|<0.5). All 12 parameters showed significant variation among the seven subpopulations, except for PHI (Appendix D).

3.3. Significant and repetitive loci associated with nutrient use efficiency traits GWAS on 12 traits

GWAS were conducted using a mixed linear model (mlm), identifying 1,451 marker-trait associations (MTAs) for 12 traits across five environments at a suggestive significance threshold of $P<1.0e^{-5}$ (Fig. 3). The overall false-positive rate was appropriately controlled, as evidenced by the Q-Q plots. Although some inflation was slightly underestimated, excessive false positives were absent (Fig. 4).

The number of MTAs per trait varied from 7 for SNUE to 675 for KUPE. Similarly, the number of QTLs ranged from 7 for SNUE to 268 for KUPE, yielding a total of 829 QTLs across all 12 traits. Environment 20SQ had the highest number of QTLs (460), whereas 20NY had the fewest (31) (Table 1). Notably, multiple nutrient use efficiency traits were commonly associated with the same QTL, reducing the total number of unique genomic regions to 534 across the wheat genome (Appendix E). These 534 significant QTLs were unevenly distributed across the three sub-genomes: 208 on the A sub-genome, 233 on the B sub-genome, and 93 on the D sub-genome. Of particular interest, more than 19.48% (104) of all QTLs were significant in at least two environments. Fourteen QTLs were detected in more than three environments (Table 2). Among these, all were located on chromosomes A and B and encompassed all 12 traits except GNUE. Notably, QTL234 on chromosome 3B was consistently associated with four traits (PHI, NHI, KUPE, and SPUE) across all five environments. Additionally, QTL335 on chromosome 5A and QTL500 on chromosome 7B were each associated with five of the 12 traits. Remarkably, KUPE showed significant associations with 13 QTLs, excluding only QTL324.

GNUE Nine single nucleotide polymorphisms (SNPs), primarily located on chromosomes 1B, 4B, 5A, 5B, and 6D, were significantly associated with GNUE. These significantly associated SNPs (SASNPs) were observed in all studied environments except 20LY. Among them, four SNPs were specifically mapped to chromosome 5A. The PVE of each

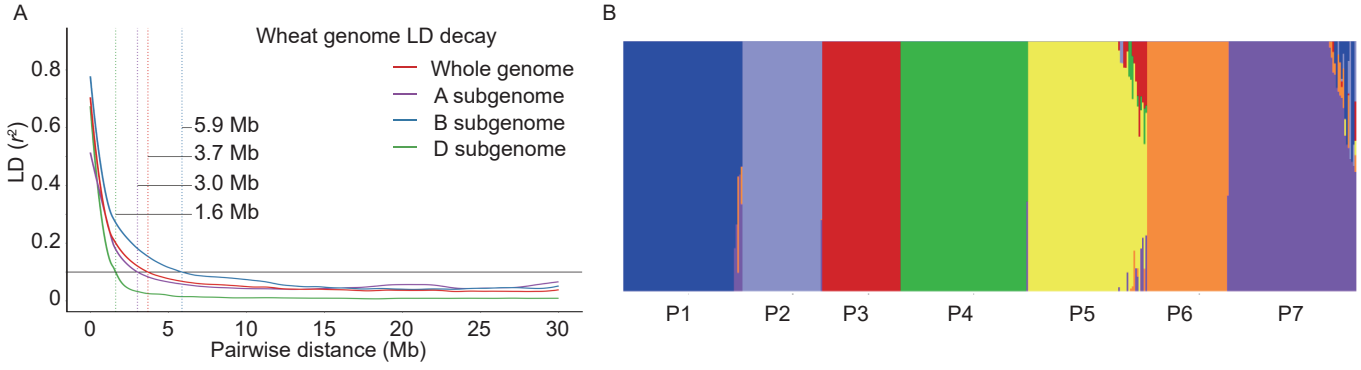


Fig. 1 Linkage disequilibrium (LD) and population structure of the single-nucleotide polymorphism (SNP) in the association panel. A, LD decay for the whole genome and A, B, and D subgenomes. B, subgroups inferred by STRUCTURE analysis.

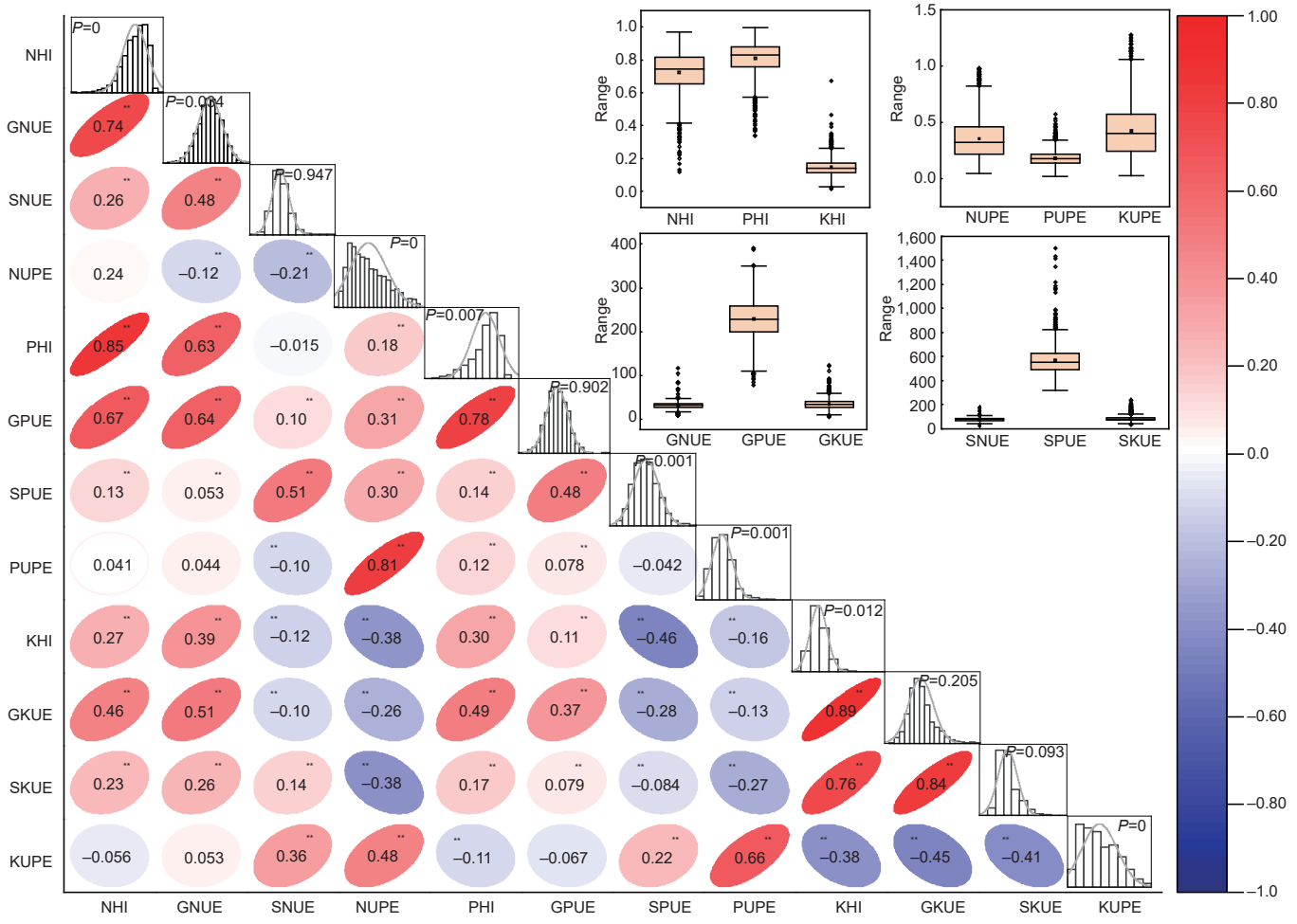


Fig. 2 Phenotype distribution of 12 traits and the correlation coefficient. The central rectangle, dividing the figure into two triangles, displays histograms for each trait. The lower triangle shows Pearson correlation coefficients (*r*-values) between pairs of traits; the upper triangle presents box-and-whisker plots illustrating trait distributions. Histogram axes represent measured phenotypic values. NHI, nitrogen harves index; GNUE, N utilization efficiency based on grain yield; SNUE, N utilization efficiency based on biomass yield; NUPE, N uptake efficiency; PHI, P harvest index; GPUE, P utilization efficiency based on grain yield; SPUE, P utilization efficiency based on biomass yield; PUPE, P uptake efficiency; KHI, K harvest index; GKUE, K utilization efficiency based on grain yield; SKUE, K utilization efficiency based on biomass yield; KUPE, K uptake efficiency. *, ** and *** denote significant differences at $P \leq 0.05$, $P \leq 0.01$ and $P \leq 0.001$, respectively, determined by Student's *t*-test.

SNP ranged from 6.05 to 8.72%. Notably, the SNP *AX-111645374* on chromosome 1B exhibited the highest LOD score (6.93) and accounted for 8.71% of phenotypic variation, indicating a positive effect on GNUE. Furthermore, the SNP marker *AX-94737971* demonstrated the largest positive effect, with an effect size of 36.38 (Tables 1 and 2; Appendix E).

NHI Seventy-six SNPs were identified, predominantly located on chromosomes 1A, 1B, 2A, 2B, 3A, 3B, 3D, 4A, 4B, 5A, 5B, 5D, 6A, 6B, 6D, 7B, and 7D, and showed significant associations with NHI. These SASNPs were consistently detected across all five environments. The PVE for each SNP ranged from 5.91 to 9.08%. Notably, SNPs *AX-111125482*, *AX-109095537*, and *AX-108919188* exhibited the highest PVE values. *AX-111125482*, positioned on chromosome 1A within QTL25, displayed a substantial PVE of 9.08%, though it had a negative effect on NHI. Indeed, most SASNPs exerted negative effects on NHI, with the exceptions of *AX-109469677* and *AX-109310979*. The LOD scores for these SNPs ranged from 5.02 to 7.29. Among them, SNPs *AX-108919188*, *AX-109095537*, and *AX-111125482* were most closely associated with NHI. Furthermore, two SASNPs — *AX-110975640* and *AX-110923966*, both within QTL387 — were simultaneously detected in the 19NY and 19YL environments (Tables 1 and 2; Appendix E).

NUPE SASNPs associated with NUPE were identified across all five environments except 19NY. A total of 56 SNPs were detected in four environments and mapped to chromosomes 1B, 1D, 2A, 2B, 3A, 4B, 5A, 5B, 6B, 7B, and 7D. The marker R^2 values for these SNPs ranged from 4.77 to 12.85%, with *AX-89767353*, *AX-109074220*, and *AX-111034350* exhibiting the highest explanatory power. Notably, all 56 SNPs had a positive effect on NUPE, with effect sizes ranging from 0.07 to 1.88. The SNPs *AX-111722493* and *AX-110520057* showed the largest effects. No QTL was consistently detected across multiple environments (Tables 1 and 2; Appendix E).

SNUE SASNPs associated with SNUE were identified in all five environments except 19LY. A total of seven SNPs were detected across the four remaining environments and were

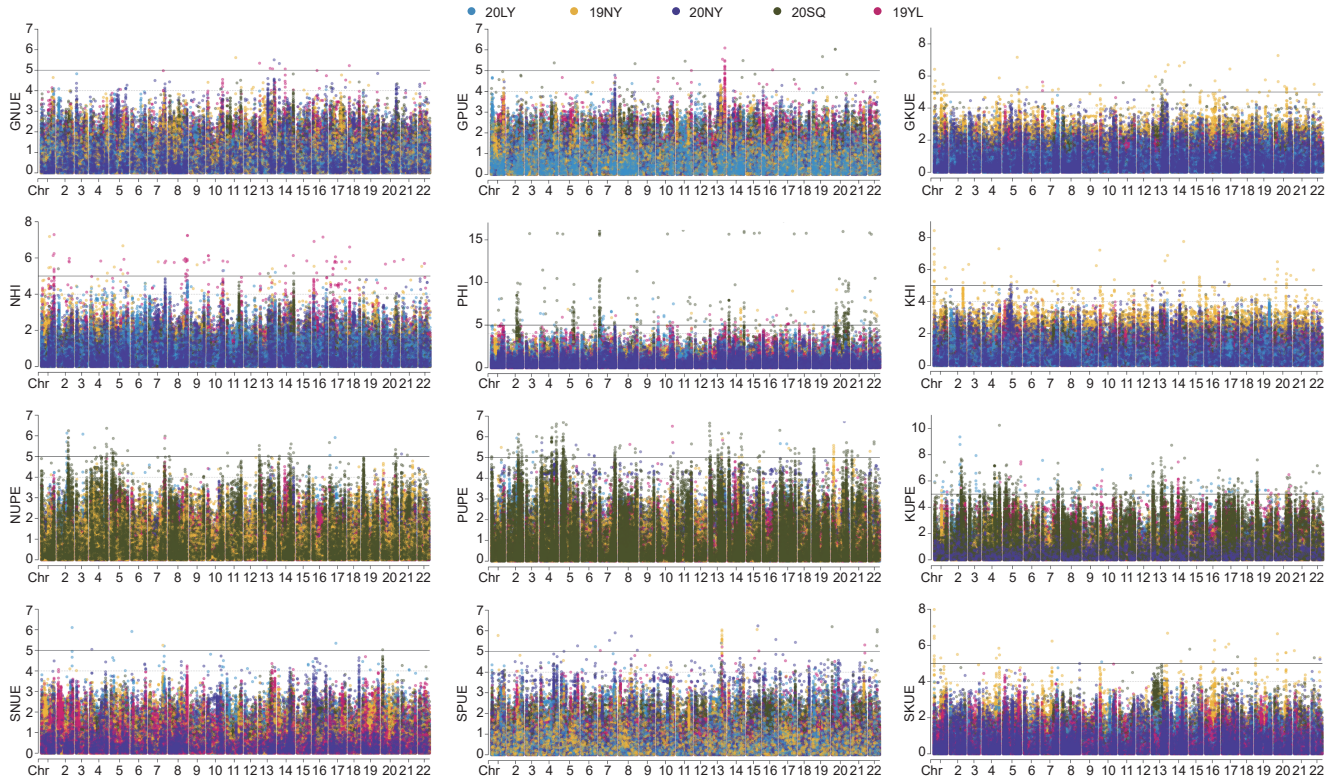


Fig. 3 Manhattan plots of marker-trait associations for 12 corrected traits related to nutrient use efficiency in the wheat panel. The *y*-axis represents $\log_{10}(P)$ values across traits, with dot colors indicating different environments. The horizontal solid line indicates the significance threshold. 20LY, the 2019–2020 growth season in Luoyang, Henan Province, China; 19NY, the 2018–2019 growth season in Nanyang; 20NY, the 2019–2020 growth season in Nanyang, Henan Province, China; 20SQ, the 2019–2020 growth season in Suqian, Jiangsu Province, China; 19YL, the 2018–2019 growth season in Yangling, Shaanxi Province, China. GNUE, N utilization efficiency based on grain yield; GPUE, P utilization efficiency based on grain yield; GKUE, K utilization efficiency based on grain yield; NHI, nitrogen harves index; PHI, P harvest index; KHI, K harvest index; NUPE, N uptake efficiency; PUPE, P uptake efficiency; KUPE, K uptake efficiency; SNUE, N utilization efficiency based on biomass yield; SPUE, P utilization efficiency based on biomass yield; SKUE, K utilization efficiency based on biomass yield.

mapped to chromosomes 1B, 2A, 2D, 3A, 6B, and 7B. The marker R^2 values for these SNPs ranged from 5.73 to 7.28%, with *AX-94786974* and *AX-111012440* exhibiting the highest explanatory power. Among the seven SNPs, five had a positive effect on SNUE, with *AX-110619644*, *AX-110574728*, and *AX-94786974* showing the largest effect sizes (Tables 1 and 2; Appendix E).

GPUE SASNPs associated with GPUE were identified in two out of the five environments tested (20SQ and 19YL), yielding a total of 18 significant SNPs. These SNPs were distributed across chromosomes 2A, 3B, 4B, 5A, 5B, 6A, 7A, and 7B. The R^2 values for individual SNPs ranged from 5.06 to 7.39%. Of the 18 SNPs, ten exhibited positive effects on GPUE, with six — detected exclusively in 20SQ — showing the highest effect sizes (Tables 1 and 2; Appendix E).

PHI SASNPs related to PHI were detected across all five environments, identifying a total of 419 SNPs distributed on all 21 chromosomes. The marker R^2 for each SNP ranged from 4.81 to 21.2%, with 21 SNPs explaining at least 20% of the phenotypic variance. Of the 419 SNPs, 319 exhibited positive effects on PHI, most of which were identified in the 20SQ environment. These 21 SNPs with the highest R^2 values also showed the largest positive effect values, ranging from 0.78 to 0.81. Notably, several SASNPs within QTL189, 190, 234, and 347 were consistently detected in two different environments (Tables 1 and 2; Appendix E).

PUPE SASNPs related to PUPE were identified across all five environments, yielding 233 significant SNPs distributed across 21 chromosomes, except chromosome 4D. The marker R^2 values for individual SNPs ranged from 5.09 to 10.6%, with *AX-109005109* exhibiting the highest value. Of the 229 SNPs analyzed, 226 showed positive effects on PUPE, with effect sizes ranging from 0.03 to 0.64. Notably, SNPs *AX-108815985*, *AX-111058597*, and *AX-111535603* displayed the largest effect sizes. Additionally, two QTLs — QTL321 and QTL338 — were detected, each encompassing multiple SNP loci. QTL321 contained three SNPs (*AX-111778392*, *AX-110369102*, and *AX-110009420*), while QTL338 included four SNPs (*AX-111655101*, *AX-109908043*, *AX-111648972*, and *AX-111070521*) (Tables 1 and 2; Appendix E).

SPUE Thirty-two SASNPs linked to SPUE were identified across all five environments. These SNPs were primarily distributed on chromosomes 1A, 2B, 2D, 3A, 3B, 5A, 6A, 6B, 7B, and 7D. The R^2 value for each SNP ranged from 5.53 to 7.84%. Among the 32 SNPs, 12 exhibited positive effects on SPUE, with effect values ranging from 102.7 to 449. Notably, several SPUE-related SNPs displayed substantially higher

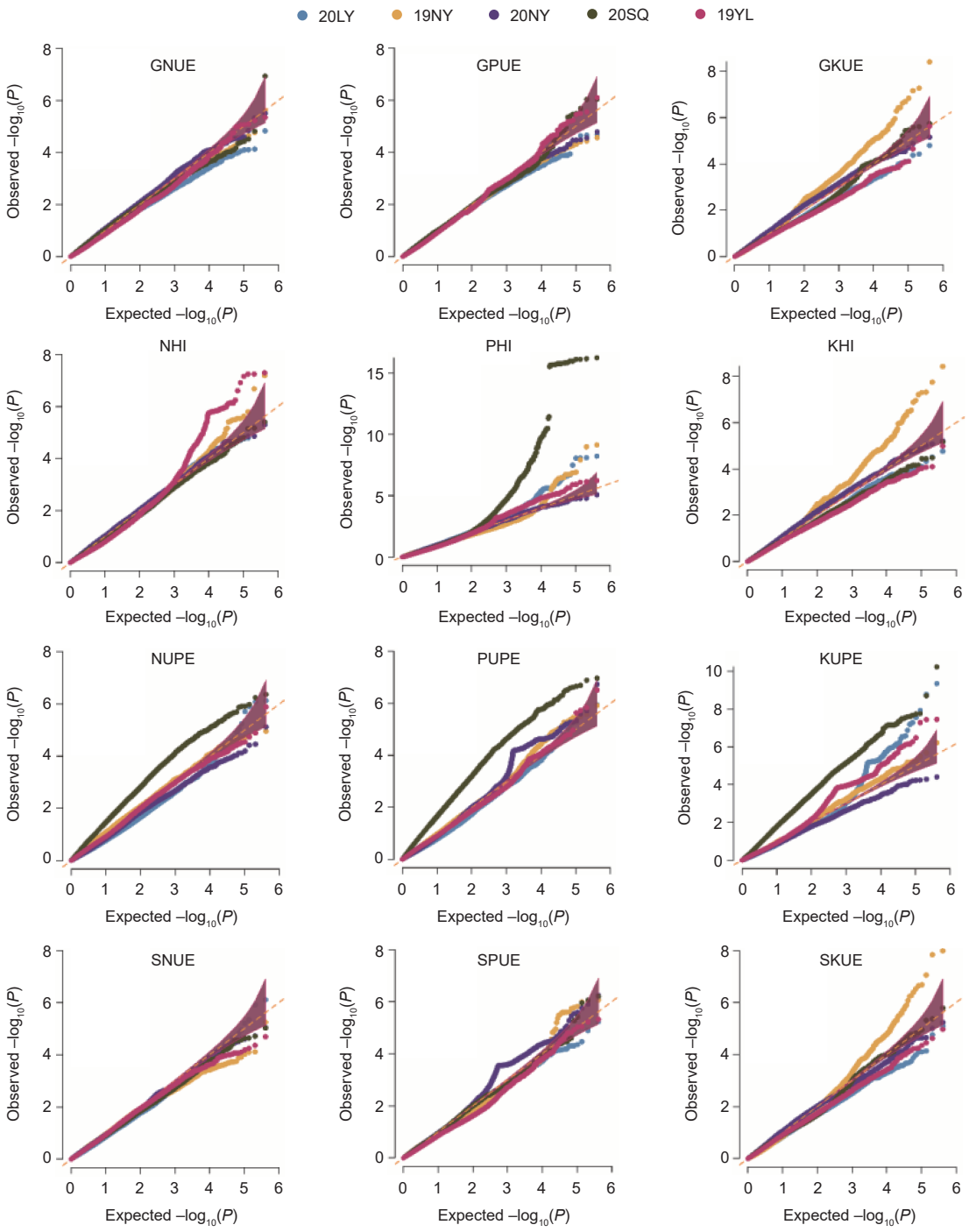


Fig. 4 Quantile-quantile (Q-Q) plots of single-nucleotide polymorphisms (SNPs) associated with 12 traits. GNUE, N utilization efficiency based on grain yield; GPUE, P utilization efficiency based on grain yield; GKUE, K utilization efficiency based on grain yield; NHI, nitrogen harvest index; PHI, P harvest index; KHI, K harvest index; NUPE, N uptake efficiency; PUPE, P uptake efficiency; KUPE, K uptake efficiency; SNUE, N utilization efficiency based on total aboveground biomass yield; SPUE, P utilization efficiency based on biomass yield; SKUE, K utilization efficiency based on biomass yield. 20LY, the 2019–2020 growth season in Luoyang, Henan Province, China; 19NY, the 2018–2019 growth season in Nanyang, Henan Province, China; 20NY, the 2019–2020 growth season in Nanyang; 20SQ, the 2019–2020 growth season in Suqian, Jiangsu Province, China; 19YL, the 2018–2019 growth season in Yangling, Shaanxi Province, China.

effect sizes compared to those observed for other traits (Tables 1 and 2; Appendix E).

GKUE SASNPs associated with GKUE were detected across all five environments, excluding 20NY, yielding 51 significant SNPs that were distributed across all 21 chromosomes except 1B, 1D, 2A, 3B, and 3D. The R^2 values for each SNPs ranged from 5.05 to 10.3%. Among the 45 SNPs analyzed, thirty-eight had positive effects on GKUE, with effect values ranging from 0.04 to 70.6. Notably, SNPs *AX-94746160* and *AX-95176602* exhibited the highest effect values. LOD scores ranged from 5.02 to 8.41, with SNP *AX-109834632* exhibiting the strongest association with GKUE, featuring

Table 1 Number of quantitative trait loci (QTLs) identified for 12 nutrient use efficiency traits by genome-wide association study (GWAS)

Trait[1)]	MTA[2)]	QTLs[3)]	No. of environments[4)]					Sub-genome[5)]		
			20LY	19NY	20NY	20SQ	19YL	A	B	D
GNUE	9	9	–	1	2	1	5	4	4	1
NHI	76	61	2	11	1	3	44	25	31	5
NUPE	56	41	6	–	1	33	1	11	27	3
SNUE	7	7	4	1	1	1	–	3	3	1
GPUE	18	11	–	–	–	6	5	6	5	–
PHI	419	185	31	15	1	125	21	61	92	32
PUPE	233	128	7	8	11	100	4	59	55	14
SPUE	32	19	1	3	9	2	4	8	6	5
GKUE	51	42	–	35	2	4	1	22	13	7
KHI	50	35	–	31	3	1	–	14	16	5
KUPE	675	268	70	7	–	182	21	106	123	39
SKUE	33	23	1	20	–	2	–	13	7	3
Total	1659	829	122	132	31	460	106	332	382	115

[1)] GNUE, grain N utilization efficiency; NHI, N harvest index; NUPE, N uptake efficiency; SNUE, shoot N utilization efficiency; GPUE, grain P utilization efficiency; PHI, P harvest index; PUPE, P uptake efficiency; SPUE, shoot P utilization efficiency; GKUE, grain K utilization efficiency; KHI, K harvest index; KUPE, K uptake efficiency; SKUE, shoot K utilization efficiency.
[2)] Number of significant marker-trait associations (MTAs) identified. 20LY, the 2019–2020 growth season in Luoyang, Henan Province, China; 19NY, the 2018–2019 growth season in Nanyang, Henan Province, China; 20NY, the 2019–2020 growth season in Nanyang; 20SQ, the 2019–2020 growth season in Suqian, Jiangsu Province, China; 19YL, the 2018–2019 growth season in Yangling, Shaanxi Province, China.
[3)] Number of identified QTLs.
[4)] Number of QTLs identified under one to eight environments; – indicates the trait phenotypes were not available. There is overlap of QTLs located between environments.
[5)] Number of QTLs in each sub-genome.

Table 2 Quantitative trait loci (QTLs) identified in more than three environments

QTL ID	Environment[1)]	Trait[2)]	Chromosome	Position (cM)
QTL11	19NY, 20LY, 20SQ	GKUE, KUPE, PHI	1A	328.09–329.48
QTL25	19YL, 19NY, 20LY	KUPE, NHI, PHI, KHI	1A	571.56–574.48
QTL80	19NY, 20NY, 20SQ	SNUE, PUPE, KUPE, KHI	2A	72.81–74.24
QTL103	20LY, 20NY, 20SQ	KUPE, PUPE, GPUE	2A	637.99–640.23
QTL211	19YL, 20NY, 20SQ	NUPE, PHI, KUPE, SPUE	3A	717.65–720.22
QTL213	19NY, 19YL, 20SQ	KUPE, NHI, GKUE, KHI	3A	737.48–739.56
QTL234	19NY, 19YL, 20NY, 20LY, 20SQ	PHI, NHI, KUPE, SPUE	3B	823.81–829.13
QTL319	19YL, 20LY, 20SQ	KUPE, PUPE, SPUE, PHI	5A	536.24–537.36
QTL324	19YL, 19NY, 20NY	GKUE, NHI, SPUE	5A	569.29–571.47
QTL335	19NY, 19YL, 20LY	NHI, GPUE, KHI, GKUE, SKUE	5A	705.54–707.15
QTL338	20LY, 20NY, 20SQ	PHI, PUPE, KUPE	5B	23.68–28.64
QTL387	19NY, 19YL, 20LY	NHI, KUPE	6A	32.87–33.56
QTL422	19YL, 20LY, 20SQ	SNUE, NHI, KUPE	6B	280.30–285.88
QTL500	19NY, 19YL, 20SQ	KHI, PHI, NHI, KUPE, PUPE	7B	535.53–540.80

[1)] 20LY, the 2019–2020 growth season in Luoyang, Henan Province, China; 19NY, the 2018–2019 growth season in Nanyang, Henan Province, China; 20NY, the 2019–2020 growth season in Nanyang; 20SQ, the 2019–2020 growth season in Suqian, Jiangsu Province, China; 19YL, the 2018–2019 growth season in Yangling, Shaanxi Province, China.
[2)] GKUE, grain K utilization efficiency; KUPE, K uptake efficiency; PHI, P harvest index; NHI, N harvest index; KHI, K harvest index; SNUE, shoot N utilization efficiency; PUPE, P uptake efficiency; GNUE, grain N utilization efficiency; GPUE, grain P utilization efficiency; NUPE, N uptake efficiency; SPUE, shoot P utilization efficiency; SKUE, shoot K utilization efficiency.

both the highest R^2 value and a relatively high positive effect value (Tables 1 and 2; Appendix E).

KHI SASNPs related to KHI were identified in two out of five environments (19NY and 20SQ), yielding a total of 50 SNPs distributed across all 21 chromosomes except 2D, 3B, 4B, 4D, 6A, and 6D. The marker R^2 values for these SNPs ranged from 5.43 to 8.68%. Several SNPs exhibited similar marker R^2 values. Notably, *AX-111140423* displayed the highest R^2 but exerted a negative effect on KHI. Of the 48 SNPs analyzed, 38 showed positive effects on KHI, with additive effects ranging from 0.02 to 61.5. The SNP *AX-109834632*, detected on chromosome 7B in 19NY, had the largest positive effect. LOD scores varied between 5.00 and 8.43. *AX-109890236*, located on chromosome 1A in 19NY, was most strongly associated with KHI. No QTL was consistently detected across multiple environments (Tables 1 and 2; Appendix E).

KUPE A total of 675 SASNPs were identified, predominantly distributed across all 21 chromosomes except 20NY. The R^2 values for individual SNPs ranged from 5.05 to 9.24%. With the exception of *AX-111620460* and *AX-109469677*, all SNPs exhibited positive effects on KUPE, with effect sizes varying

from 0.04 to 0.86. LOD scores spanned from 0.5 to 10.2. Notably, SNP *AX-89767353* displayed the highest LOD value but exerted only a modest influence on KUPE. In contrast, SNP *AX-109074220*, located on chromosome 2A, showed both a relatively high LOD score and a substantial effect size. QTLs 25, 40, 144, 162, 211, 277, 345, and 347 each encompass two or more SNP loci detected in two environments (Tables 1 and 2; Appendix E).

SKUE In three out of five environments (20LY, 19NY, and 20SQ), SASNPs related to SKUE were detected. A total of 33 SASNPs were identified, distributed across all 21 chromosomes except 2D, 3B, 4B, 4D, 6A, and 6D. The marker R^2 values for these SNPs ranged from 5.00 to 8.75%. Among them, *AX-110359738* exhibited the highest R^2 and had a positive effect on SKUE. Of the 33 SNPs, 20 showed a positive effect, with effect values ranging from 0.06 to 95.11. The SNP *AX-111610738*, detected on chromosome 7B in the 19NY environment, had the largest effect value. LOD scores ranged from 5.00 to 7.98. No QTL was consistently detected across more than one environment (Tables 1 and 2; Appendix E).

3.4. Meta-analysis for wheat QTLs controlling NUE, PUE and KUE

A total of 47 meta-QTLs (MQTLs) associated with NUE, PUE, and KUE were identified, of which 34 were successfully mapped onto the physical map of the wheat reference genome (Appendix C). The remaining 13 MQTLs failed to map due to unavailable physical positions. Among the 34 mapped MQTLs, 30 were located within a physical interval of less than 20 Mb, representing 61.7% of the total MQTLs. These MQTLs are distributed across 12 wheat chromosomes: 1D, 2A, 2D, 3D, 4A, 4D, 5D, 6A, 6D, 7A, 7B, and 7D (Fig. 5). The 34 MQTLs consist of varying numbers of initial QTLs, ranging from 1 to 16, with only 18

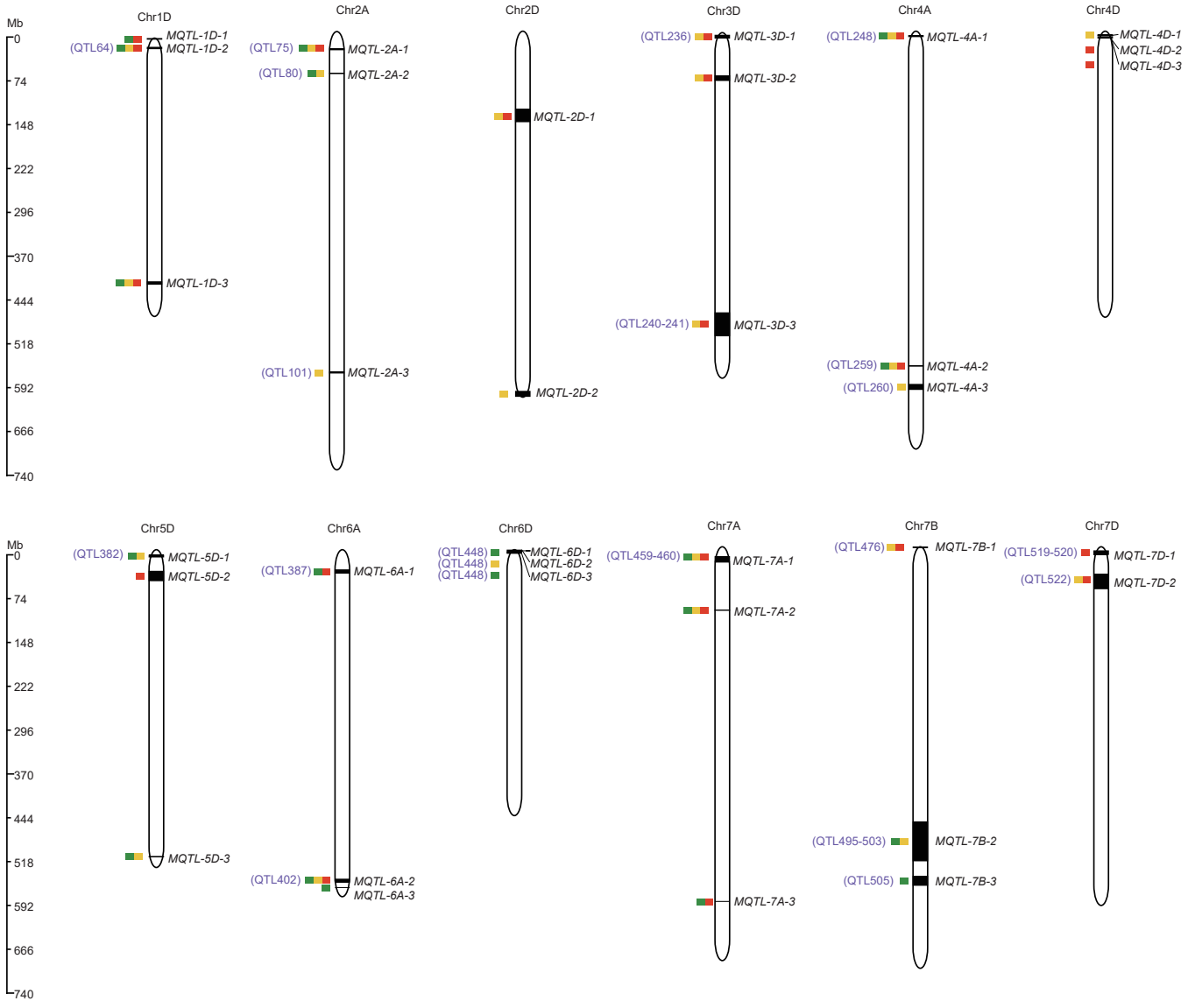


Fig. 5 Distribution of meta-quantitative trait loci (MQTLs) and the QTLs detected in genome-wide association study (GWAS). Black font (right side of chromosome figure) represents MQTLs, while QTLs from GWAS are indicated in purple font (left side). Red, yellow, and green colors represent nitrogen (N), phosphorus (P), and potassium (K) use efficiency, respectively.

of the 34 MQTLs comprising more than 10 initial QTLs. With the exception of chromosomes 7A and 7D, all other chromosomes harbored three MQTLs. Both genetic and physical positions of flanking markers for these MQTLs were determined using a consensus map. Each MQTL was associated with 1 to 8 traits related to NUE, PUE, or KUE. Seven MQTLs — MQTL-1D-2, MQTL-1D-3, MQTL-4A-1, MQTL-4A-2, MQTL-6A-2, MQTL-7A-1, and MQTL-7A-2 — were associated simultaneously with NUE, PUE, and KUE. Another seven MQTLs — MQTL-2D-1, MQTL-3D-1, MQTL-3D-2, MQTL-3D-3, MQTL-4D-2, MQTL-7B-1, and MQTL-7D-2 — co-influenced NUE and PUE. Three MQTLs — MQTL-1D-1, MQTL-6A-1, and MQTL-7A-3 — affected both NUE and KUE, while three others — MQTL-2A-2, MQTL-5D-1, and MQTL-7B-2 — impacted both PUE and KUE. MQTL-4D-3, MQTL-5D-3, and MQTL-7D-1 were exclusively associated with NUE, whereas five MQTLs — MQTL-2A-3, MQTL-2D-2, MQTL-4A-3, MQTL-4D-1, and MQTL-6D-2 — were solely linked to PUE. Five MQTLs (MQTL-6A-3, MQTL-6D-1, MQTL-6D-3, and MQTL-7B-3) exclusively impacted KUE. Five MQTLs (MQTL-6A-3), MQTL-6D-1, MQTL-6D-3, and MQTL-7B-3 — exclusively influenced KUE. An MQTL was considered co-localized with a GWAS-derived QTL if the latter resided within or near the LD span of the MQTL. A total of 21 GWAS-detected QTLs were found to be co-localized with MQTLs (Fig. 5). Among these, five MQTLs — MQTL-3D-3, MQTL-4A-3, MQTL-7B-3, MQTL-7D-1, and MQTL-7D-2 — were co-localized with QTLs (QTL240–241, QTL260, QTL505, QTL519–520, and QTL522) identified through GWAS. Notably, the specific traits associated with the MQTLs and GWAS QTLs sometimes differed. In some cases, the traits related to QTLs and MQTLs were the same. For instance, MQTL-1D-2 was related to NUE, PUE and KUE, similar to QTL64, which was associated with PUPE and KUPE. Additionally, MQTL-2A-2, MQTL-6A-1, and MQTL-7B-2 were co-localized with QTL80, QTL387, and QTL495–503, respectively, all of which were detected across more than three environments.

3.5. Haplotype analysis of NHI

In addition to loci identified in previous studies, we have discovered numerous novel QTLs associated with nitrogen, phosphorus, and potassium use efficiency. Notably, QTL234 was consistently detected across all five environments and associated with four of the twelve traits. NHI showed a robust association with the SNP markers *AX-109095537* and *AX-108919188*, both located within QTL234. These markers exhibited the highest marker R^2 values in QTL234, although they had a negative effect (–0.44) on NHI. Positioned within a 0.08 Mb region (828.67–828.76 Mb) on chromosome 3B, these SNPs were subjected to haplotype analysis, revealing three LD blocks that primarily comprised seven haplotypes (Fig. 6-A–D). Haplotypes 1 through 7 included 89, 30, 93, 40, 26, 12, and 18 accessions, respectively. Among them, Hap-7 exhibited the highest NHI across all environments except NY-19. In three environments (LY-20, NY-19, and YL-19), Hap-5 showed significantly lower NHI compared to the other haplotypes (Fig. 6-E). Hap-1 to Hap-6 displayed higher sequence similarity but differed significantly from Hap-7 (Fig. 6-E and F).

3.6. Candidate genes in co-located and novel region

QTL80 (72.12061–74.241884 Mb, located on chromosome 2A), QTL387 (32.872277–33.556442 Mb, located on chromosome 6A), and QTL500 (535.532725–540.797948 Mb, located on chromosome 7B) were consistently identified as significant across more than three environmental conditions in this study (Fig. 5; Table 2). These QTLs co-localize within the MQTL region and have therefore been designated as co-located candidate gene regions. QTL80, QTL387, and QTL500 encompass 27, 18, and 45 high-confidence candidate genes, respectively. Among these 90 genes, 50 showed no detectable expression or exhibited extremely low expression levels in wheat, whereas the remaining 40 were expressed in various combinations across different wheat tissues, including roots, stems, leaves, spikes, and grains (Appendix F). Of these 40 expressed genes, 26 belonged to protein families such as ribose-phosphate pyrophosphokinase, membrane-associated zinc metalloprotease family protein, and zinc finger CCCH domain-containing protein. Two genes were annotated as transcription factors — specifically, a bZIP transcription factor and elongation factor 1-beta. To elucidate the functional roles of these 90 candidate genes, a Gene Ontology (GO) enrichment analysis was conducted, categorizing them into BP, molecular function (MF), and cellular component (CC) domains (Appendix G). Most genes were associated with binding and catalytic activity under MF; from the BP perspective, they were enriched in cellular processes, metabolic processes, and responses to stimuli. In terms of CC, the genes were predominantly linked to cell part, cell, membrane, organelle, organelle part, protein-containing complex, and membrane. Furthermore, KEGG pathway analysis revealed that these genes were enriched in ubiquinone and other terpenoid-quinone biosynthesis, ribosome biogenesis in eukaryotes, selenocompound metabolism, and biosynthesis of secondary metabolites (Appendix H).

QTL234 (823.811169–829.133497 Mb, located on chromosome 3B) emerged as a novel region identified across all five environments in this study. This QTL was associated with PHI, NHI, KUPE, and SPUE (Fig. 5; Table 2). Within the QTL234 interval, we identified 57 high-confidence candidate genes. Of these, 39 displayed negligible or extremely low expression levels in wheat, while the remaining 18 were expressed in various wheat organs (Appendix I). Notably, among the 18 expressed genes, 12 were classified into protein families including dof zinc finger protein, ankyrin repeat family protein, and ABC transporter B family protein. Additionally, six genes encoded enzymes belonging to the GDSL esterase/lipase, cytochrome P450, and pectin acetyl esterase families. Functionally, most of these genes were associated with catalytic activity and binding from the MF standpoint, and from the BP perspective, they were involved in cellular processes, metabolic processes, cellular component organization or biogenesis, regulation of biological processes, and biological regulation. With respect to CC, these genes were localized to cell part, organelle, membrane part, and membrane (Appendix J). Moreover,

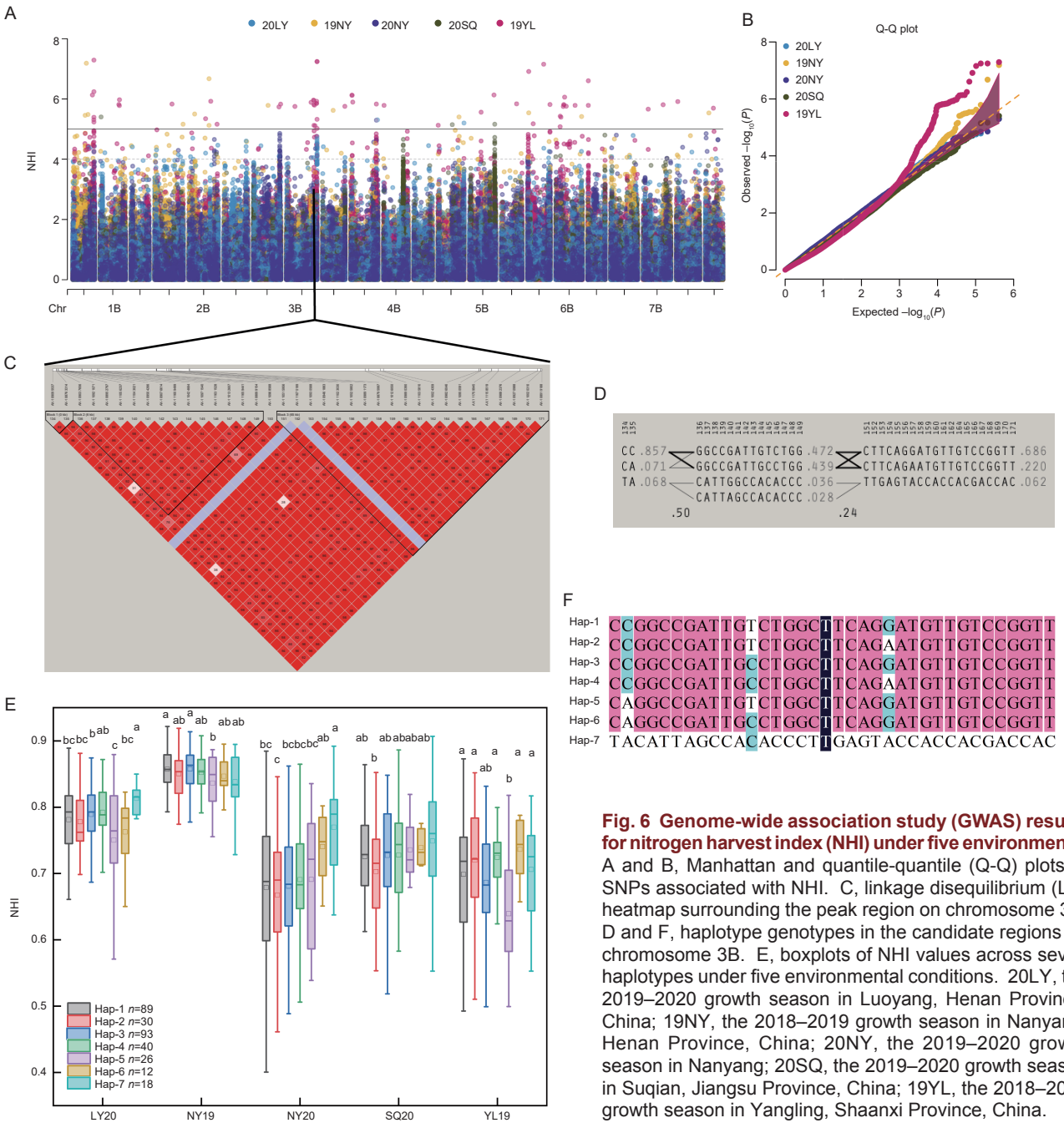


Fig. 6 Genome-wide association study (GWAS) results for nitrogen harvest index (NHI) under five environments. A and B, Manhattan and quantile-quantile (Q-Q) plots of SNPs associated with NHI. C, linkage disequilibrium (LD) heatmap surrounding the peak region on chromosome 3B. D and F, haplotype genotypes in the candidate regions on chromosome 3B. E, boxplots of NHI values across seven haplotypes under five environmental conditions. 20LY, the 2019–2020 growth season in Luoyang, Henan Province, China; 19NY, the 2018–2019 growth season in Nanyang, Henan Province, China; 20NY, the 2019–2020 growth season in Nanyang; 20SQ, the 2019–2020 growth season in Suqian, Jiangsu Province, China; 19YL, the 2018–2019 growth season in Yangling, Shaanxi Province, China.

KEGG pathway analysis of these 57 genes indicated enrichment in linoleic acid metabolism, ABC transporters, and spliceosome pathways (Appendix K).

3.7. Development of dCAPS markers on *AX-109095537*

The SNP *AX-109095537*, which exhibited a high LOD value (7.2) and was associated with NHI within QTL234, is located in an exon of *TraesCS3B01G904700LC.1*. This gene encodes a reverse-transcriptase zinc-binding domain protein, suggesting potential functional significance. Therefore, SNP *AX-109095537* was selected for the development of a derived cleaved amplified polymorphic sequence (dCAPS) marker. Following two rounds of PCR amplification, a 502 BP sequence was successfully amplified. The restriction enzyme *Bsm*AI (5′-GTCTCN-3′) was chosen for digestion of the PCR product. In wheat varieties carrying a T at this locus, such as Chinese Spring, the amplified product is cleaved by *Bsm*AI into fragments of 268 and 134 bp. In contrast, in wheat lines with a C allele — including Nongda 36, Xiaohongmai, and Xiaoyan 759 — the amplified product lacks the *Bsm*AI recognition site, resulting in no cleavage (Fig. 7).

4. Discussion

4.1. Genetic variation of nutrient use efficiency parameters of wheat

In our study, the ranges of N, P, and K use efficiency parameters were expanded or narrowed (Fig. 2). Genetic variation in these traits among wheat cultivars has been extensively documented (Hawkesford 2017; Lin *et al.*

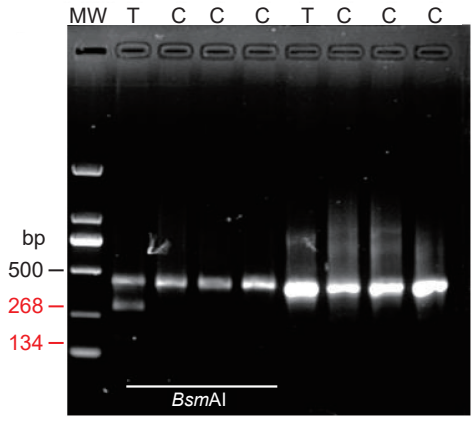


Fig. 7 Specific DNA bands generated by restriction enzyme digestion. MW, molecular weight.

2020). It is important to note that nutrient use efficiency-related parameters are influenced by multiple factors, and the determination of their ranges depends on the number of genotypes studied, fertilizer application rates, and prevailing environmental conditions. The size of the investigated population and the degree of genetic background similarity affect the scope of these indicators. For example, GNUE ranged from 0 to 30 kg kg^{-1} among 299 current and historical Great Plains hard winter wheat cultivars as reported in Guttieri *et al*. (2017), whereas it ranged from 27 to 77 kg kg^{-1} among 32 elite commercial cultivars in Barraclough *et al*. (2010), indicating substantial differences between the two populations. Additionally, Silva *et al.* (2020) provided a global perspective on NUE trends in wheat, showing a GNUE range of 17 to 112 kg kg^{-1}, similar to our findings, which reflects the diverse genetic background of the wheat cultivars evaluated. Our results also expanded the observed range of NHI across 431 wheat cultivars compared to small population, showing varying ranges, such as 0.73 to 0.83, 0.79 to 0.86, and 0.69 to 0.98 among 6, 21, and 36 cultivars, respectively (Barraclough *et al.* 2010; Górny *et al.* 2011; Liang *et al.* 2014). Similarly, our study revealed a broader range of SPUE values compared to previous studies involving 10 and 100 wheat cultivars (McDonald *et al.* 2018, He 2003). In comparison with a prior study using 11 wheat cultivars (Yang *et al*. 2022), our analysis identified a wider range of PHI values across 431 cultivars. These findings indicate that our germplasm possesses a broad genetic base and rich genetic diversity. Fertilizer input influences nutrient uptake efficiency. As shown in our study, the lower limit of NUPE was lower than those reported in previous studies, ranging from 0.4 to 1.2 kg kg^{-1} (Gaju *et al.* 2016; Frels *et al.* 2018). Furthermore, both the lower and upper limits of PUPE in our study (0.02 to 0.57 kg kg^{-1}) were lower than those in a previous report of 0.11 to 6.47 kg kg^{-1} among eight wheat cultivars (Meier *et al*. 2022). This discrepancy may be attributed to excessive application of nitrogen and phosphorus fertilizers in our experiments. Some previous studies have investigated the variation in nutrient use efficiency of wheat under greenhouse conditions. For instance, Zhang *et al*. (2019) reported GPUE ranging from 15.93 to 66.91 kg kg^{-1} among eight spring wheat cultivars, a narrower range compared to results from Manske *et al*. (2001), Su *et al.* (2009), Yang *et al*. (2022), and our field-based study.

4.2. The QTLs related with nutrient use efficiency of wheat

Our study demonstrates the involvement of multiple loci in complex N, P, and K use efficiency (Appendix E), consistent with previous findings (Liu *et al.* 2021; Bandyopadhyay *et al.* 2022). Over the past 15 years, a large number of QTL mapping data for NUE, PUE, and KUE — along with associated traits — have advanced understanding of the genetic basis underlying N, P, and K utilization in wheat (Cormier *et al*. 2014). Through GWAS, Shi *et al.* (2022) identified 11 stable QTLs for low-N tolerance indices, among which qFsnR5A.2 (fertile spikelet number), qSLR6D.1 (spike length), and qGYPR2A.3 (grain yield per plant) co-localized with QTL314, QTL448, and QTL115 in our study, respectively. Notably, QTL448, associated with both PUE- and KUE -related traits, co-localized with MQTL-6D-1, MQTL-6D-2, and MQTL-6D-3 (Fig. 5), underscoring its role as a key genomic region influencing N, P, and K use efficiency. A prior GWAS identified qCIR1A.5, linked to an NUE-related trait (chlorate inhibition rate), which also co-localizes with QTL25-associated with N, P, and K use efficiency in our study (Shi *et al*. 2023). These convergent results, both historical and current, reveal loci that influence multiple nutrient efficiency traits, suggesting coordinated uptake and utilization of N, P, and K during wheat development. Guo *et al*. (2012) reported 32 genomic regions governing simultaneous nutrient uptake and utilization, encompassing 190 individual QTLs, further supporting shared genetic control across N, P, and K efficiency. QTLs associated with N–P interaction effects were detected on chromosomes 1D, 3A, 4B, and 6A (Xu *et al*. 2014). Additionally, Han *et al*. (2023) identified QGka/Stpue on chromosome 4B, which was associated with PUE and KUE related traits simultaneously. However, these earlier studies lacked precise marker positions, limiting direct comparison with our QTLs. In this work, we identified 14 QTLs associated with N, P, and K use efficiency-related traits across more than three environments (Table 2), potentially reflecting either tightly linked QTLs or pleiotropic effects (Wang *et al.* 2007).

Meta-QTL analysis integrates diverse QTL datasets while accounting for differences in genetic background, phenotypic variation, and environmental conditions (Said *et al*. 2013), thereby refining confidence intervals. Genomic regions where MQTLs overlap with GWAS signals represent strong candidates for improving wheat nutrient use efficiency and serve as strategic targets for breeding programs. In this study, 30 MQTLs were mapped to genomic intervals smaller than 20 Mb (Appendix C). Notably, MQTL-4A-1 (25.84–28.79 cM), previously associated with root N content, root K content, shoot K content, and root K use efficiency (Saini *et al.* 2021), overlaps with MQTL-4 (22.5–37.5 cM), identified here as associated with NUE traits. GWAS results provide empirical support for MQTLs, enhancing their reliability. Here, over 60% of MQTLs (21/34) co-localized with our

GWAS signals (Fig. 5). Among them, MQTL-1D-2 (QTL64), MQTL-2A-2 (QTL80), and MQTL-6D-1 (QTL448) exhibited overlapping positions with MQTL1D.3 (10.66–423.3 cM), MQTL2A.2a (25.6–43.3 cM), and MQTL6D.1 (0.06–1.57 cM), respectively — all previously linked to NUE-related traits (Saini *et al.* 2021). QTL448 has been repeatedly detected across independent studies, reinforcing its significance. Only three QTLs (QTL80, QTL387, and QTL500) that co-localized with MQTLs were detected in more than three environments, indicating stability in their effects on nutrient use efficiency under varying conditions (Alemu *et al*. 2021). These co-localized regions therefore represent high-priority targets for marker-assisted selection within wheat breeding initiatives (Yang Y *et al.* 2021).

4.3. Candidate genes related with nutrient use efficiency of wheat

The integration of GWAS and MQTL analyses identified 90 high-confidence candidate genes associated with nutrient use efficiency (NUE) (Appendix F). Within the QTL500 region, a bZIP transcription factor gene, *TraesCS7B02G299200*, was detected on chromosome 7B. Members of the *TabZIP14-B* gene family have been reported to play essential roles in salt and freezing tolerance as well as resistance to stripe rust in wheat (Zhang *et al*. 2008, 2017). Previous studies indicate that another bZIP transcription factor, *TabZIP60*, located on chromosome 6D, negatively regulates both plant growth and nitrogen use efficiency (Yang *et al*. 2019). More recently, Mueth and Hulbert (2022) suggested that *TraesCS7B02G299200* may participate in the regulation of wheat stripe rust resistance. However, the functional role of *TraesCS7B02G299200* in nitrogen, phosphorus, or potassium uptake and utilization remains unknown. A potassium transporter gene (*HAK*) was identified within QTL387, which is associated with KUPE. Currently, only *TaHAK1*, *TaHAK5* and *TaHAK17* have been experimentally confirmed to mediate low-affinity K^+ uptake in wheat (Cheng *et al.* 2018). Additionally, several genes encoding serine/threonine protein kinases were localized to chromosome 7B. Notably, a serine/amino acid protein kinase gene on chromosome 4D has been shown to phosphorylate *TaCol-B5*, leading to increased spikelet number and spike length, resulting in a 19% improvement in grain yield (Zhang *et al*. 2022).

QTL234 represents a novel genomic region associated with nitrogen, phosphorus, and potassium use efficiency in this study. Seven haplotypes were observed within QTL234 across a panel of 431 wheat cultivars. These haplotypes exhibited significant differences in N, P, and K use efficiency and spanned 57 high-confidence candidate genes (Fig. 6-E; Appendix I). Among them, *TraesCS3B02G608800* encodes a DOF zinc finger protein previously implicated in the regulation of stem pith cell apoptosis (Liu *et al*. 2023). Importantly, this gene has also been linked to nitrogen use efficiency in prior research, though its molecular mechanism in nutrient utilization requires further investigation. Most plant ankyrin repeat (ANK) proteins function in defense responses and, in some cases, in growth and development, due to their ability to mediate protein–protein interactions (Vo *et al*. 2015). In wheat, Kolodziej *et al.* (2021) identified *Lr14a-7BL*, which encodes a protein containing 12 ankyrin repeats and six predicted transmembrane helices, highlighting the involvement of Ankyrin repeat family (ANK)-transmembrane-like proteins in race-specific disease resistance. Nevertheless, it remains unclear whether ANK proteins in wheat respond to deficiencies in nitrogen, phosphorus, or potassium. Another gene identified in this study, *TraesCS3B02G609600*, encodes a cytochrome P450 enzyme. Cytochrome P450s are multifunctional oxidases involved in biosynthetic pathways and metabolic detoxification in plants, contributing to defense against pathogen attack (Mizutani and Sato 2011). In wheat, P450 enzymes participate in detoxification processes, secondary metabolism, and various oxidation and hydroxylation reactions (Pinot *et al.* 1994; Forthoffer *et al.* 2001). Recent transcriptome analysis in *Panax notoginseng* revealed that 10 cytochrome P450 genes were significantly up-regulated and 37 significantly down-regulated under low nitrogen conditions (Xiong *et al*. 2021), underscoring the potential regulatory role of this gene family in nutrient efficiency. Furthermore, Li *et al*. (2010) identified a wheat *P450* gene closely associated with Fusarium head blight resistance, showing an expression level 84-fold higher in the resistant variety Sumai 3 compared to the susceptible Annong 8455. Despite these findings, most wheat P450 proteins remain poorly characterized at the functional level.

4.4. Molecular breeding of wheat cultivars with high nutrient use efficiency

In this study, the SNP *AX-109095537*, which exhibited a high LOD value (7.2) within QTL234 associated with NHI, was converted into a derived restriction endonuclease polymorphic sequence (dCAPS) marker (Fig. 7). SASNPs identified within QTL regions represent valuable tools for marker-assisted selection, facilitating genetic improvement of target traits. Both restriction site amplified polymorphic sequence (CAPS) and dCAPS markers, as codominant SNP-based systems, are widely employed in crop breeding due to their low cost, operational simplicity, minimal DNA requirements, and reliable inheritance patterns. Previous studies have successfully developed and validated functional SNP markers linked to yield-related traits (Hao *et al.* 2024). For example, the CAPS marker TaGW-4B was developed and validated across 205 wheat varieties, demonstrating a highly significant association with 1,000-grain weight, underscoring its utility in efficient marker-assisted selection (Duan *et al*. 2020). In another study by Li *et al*. (2016), SNP1(A/G) and SNP2(T/C) located in the promoter region (at positions 207 and 1,696 bp) of TaLTP-s were converted into dCAPS markers. The authors reported that genotypes carrying the G allele produced significantly more spikes per plant compared to A homozygotes, while those with the C allele exhibited significantly greater plant height. Huang *et al*. (2020) cloned the coding sequences of wheat *TaNRT12L12* from the A, B, and D genomes and identified three haplotypes associated with plant height, spikelet number, and thousand-grain weight for both *TaNRT12L12-A* and *TaNRT12L12-B* using SNP-

based dCAPS markers. CAPS and dCAPS markers have also been applied to assess grain quality traits. For instance, a CAPS marker for Q^{c1}-N8, associated with yield and grain protein content, was developed (Chen *et al*. 2022). Jing *et al*. (2022) developed the TaSPP-5A-dCAPS marker, which correlates with sucrose content. Additionally, the *Rht8* gene, which regulates plant height, was converted into the functional CAPS-Rht8 marker for genotyping. That study revealed that 32.6% of wheat materials carried short-stem alleles at the Rht8 locus, whereas 67.4% contained tall-stem alleles (Chai *et al*. 2022). Applications of CAPS and dCAPS markers in improving nutrient use efficiency in wheat breeding have also been documented. Notably, a CAPS marker (TaGS1a-CAPS) was developed in Chinese spring wheat to predict nitrogen, phosphorus, and potassium concentrations, as well as grain size traits, based on allele presence or absence (Guo *et al*. 2013). This study provides genetic resources for wheat nutrient utilization and has established molecular markers of practical value for enhancing NUE-related traits, particularly NHI.

5. Conclusion

A comprehensive GWAS was conducted using data from five multi-environment field trials, encompassing 12 nutrient use efficiency traits evaluated in a diverse panel of both adapted and exotic bread wheat lines. A total of 534 QTLs associated with nutrient use efficiency were detected across the entire wheat genome for these 12 traits. Fourteen QTLs related to NUE, PUE and KUE were identified in more than three environments through GWAS. By integrating GWAS results with meta-QTL analysis, three stable co-localized QTLs and one novel QTL influencing N, P, and K use efficiency were identified. These findings suggest that individual QTLs may pleiotropically influence multiple nutrient use efficiency traits. The genomic regions harboring these QTLs contain 90 and 57 candidate genes, including a *bZIP* transcription factor, a potassium transporter gene, and ANK proteins. However, the functional roles and regulatory mechanisms of these genes in nutrient use efficiency require further experimental validation. Additionally, the dCAPS marker of SNP *AX-109095537*, associated with NHI, provides a valuable tool for marker-assisted selection in wheat breeding programs targeting improved NHI. Collectively, the results of this study provide novel insights into the genetic architecture underlying nutrient use efficiency in bread wheat, offering potential targets for future breeding strategies aimed at enhancing nutrient utilization efficiency.

Acknowledgements

The work was funded by the National Key R&D Program of China (2021YFD1900700).

Declaration of competing interest

The authors declare that they have no conflict of interest.

Declaration of generative AI and AI-assisted technologies in the writing processs

During the preparation of this manuscript, the authors used ChatGPT 4.0 to assist in improving the clarity and readability of the language. All content generated was carefully reviewed and revised by the authors as necessary, and the authors take full responsibility for the final content of the article.

Appendices associated with this paper are available at https://doi.org/10.1016/j.jia.2024.06.012

References

Alemu G, Dabi A, Geleta N, Duga R, Solomon T, Zegaye H, Getamesay A, Delesa A, Asnake D, Asefa B, Shewaye Y, Abeyo B G, Badebo A. 2021. Genotype×environment interaction and selection of high yielding wheat genotypes for different wheat-growing areas of Ethiopia. *American Journal of BioScience*, **9**, 63–71.

Arcade A, Labourdette A, Falque M, Mangin B, Chardon F, Charcosset A, Joets J. 2004. BioMercator: integrating genetic maps and QTL towards discovery of candidate genes. *Bioinformatics*, **20**, 2324–2326.

Arjona J M, Royo C, Dreisigacker S, Ammar K, Villegas D. 2018. Effect of *Ppd-A1* and *Ppd-B1* allelic variants on grain number and thousand kernel weight of durum wheat and their impact on final grain yield. *Frontiers in Plant Science*, **9**, 888.

Bandyopadhyay T, Swarbreck S M, Jaiswal V, Maurya J, Gupta R, Bentley A R, Griffiths H, Prasad M. 2022. GWAS identifies genetic loci underlying nitrogen responsiveness in the climate resilient C_4 model *Setaria italica* (L.). *Journal of Advanced Research*, **42**, 249–261.

Barraclough P B, Howarth J R, Jones J, Lopez-Bellido R, Parmar S, Shepherd C E, Hawkesford M J. 2010. Nitrogen efficiency of wheat: Genotypic and environmental variation and prospects for improvement. *European Journal of Agronomy*, **33**, 1–11.

Brasier K, Ward B, Smith J, Seago J, Oakes J, Balota M, Davis P, Fountain M, Brown-Guedira G, Sneller C, Thomason W, Griffey C. 2020. Identification of quantitative trait loci associated with nitrogen use efficiency in winter wheat. *PLoS ONE*, **15**, e0228775.

Chai L, Xin M, Dong C, Chen Z, Zhai H, Zhuang J, Cheng X, Wang N, Geng J, Wang X, Bian R, Yao Y, Guo W, Hu Z, Peng H, Bai G, Sun Q, Su Z, Liu J, Ni Z. 2022. A natural variation in Ribonuclease H-like gene underlies *Rht8* to confer "Green Revolution" trait in wheat. *Molecular Plant*, **15**, 377–380.

Chen Q, Guo Z R, Shi X L, Wei M Q, Fan Y Z, Zhu J, Zheng T, Wang Y, Kong L, Deng M, Cao X Y, Wang J R, Wei Y M, Jiang Q T, Jiang Y F, Chen G Y, Zheng Y L, Qi P F. 2022. Increasing the grain yield and grain protein content of common wheat (*Triticum aestivum*) by introducing missense mutations in the Q gene. *International Journal of Molecular Sciences*, **23**, 10772.

Cheng X Y, Liu X D, Mao W W, Zhang X R, Chen S L, Zhan K H, Bi H H, Xu H X. 2018. Genome-wide identification and analysis of HAK/KUP/KT potassium transporters gene family in wheat (*Triticum aestivum* L.). *International Journal of Molecular Sciences*, **19**, 3969.

Cormier F, Le Gouis J, Dubreuil P, Lafarge S, Praud S. 2014. A genome-wide identification of chromosomal regions determining nitrogen use efficiency components in wheat (*Triticum aestivum* L.). *Theoretical and Applied Genetics*, **127**, 2679–2693.

Cui F, Fan X, Zhao C, Zhang W, Chen M, Ji J, Li J. 2014. A novel genetic map of wheat: Utility for mapping QTL for yield under different nitrogen treatments. *BMC Genetics*, **15**, 57.

Darvasi A, Soller M. 1997. A simple method to calculate resolving power and confidence interval of QTL map location. *Behavior Genetics*, **27**, 125–132.

Darzi-Ramandi H, Shariati V J, Tavakol E, Najafi-Zarini H, Bilgrami S S, Razavi K. 2017. Detection of consensus genomic regions associated with root architecture of bread wheat on groups 2 and 3 chromosomes using QTL meta-analysis. *Australian Journal of Crop Science*, **111**, 777–785.

Duan X, Yu H, Ma W, Sun J, Zhao Y, Yang R, Ning T, Li Q, Liu Q, Guo T, Yan M, Tian J, Chen J. 2020. A major and stable QTL controlling wheat thousand grain weight: Identification, characterization, and CAPS marker development. *Molecular Breeding*, **40**, 68.

Earl D A, Vonholdt B M. 2012. STRUCTURE HARVESTER: A website and program for visualizing STRUCTURE output and implementing the Evanno method. *Conservation Genetics Resources*, **4**, 359–361.

Forthoffer N, Helvig C, Dillon N, Benveniste I, Zimmerlin A, Tardif F, Salaun J P. 2001. Induction and inactivation of a cytochrome P450 confering herbicide resistance in wheat seedlings. *European Journal of Drug Metabolism and Pharmacokinetics*, **26**, 9–16.

Frels K, Guttieri M, Joyce B, Leavitt B, Baenziger P S. 2018. Evaluating canopy spectral reflectance vegetation indices to estimate nitrogen use traits in hard winter wheat. *Field Crops Research*, **217**, 82–92.

Gaju O, DeSilva J, Carvalho P, Hawkesford M J, Griffiths S, Greenland A, Foulkes M J. 2016. Leaf photosynthesis and associations with grain yield, biomass and nitrogen-use efficiency in landraces, synthetic-derived lines and cultivars in wheat. *Field Crops Research*, **193**, 1–15.

Giordano N, Sadras V O, Lollato R P. 2023. Late-season nitrogen application increases grain protein concentration and is neutral for yield in wheat. A global meta-analysis. *Field Crops Research*, **290**, 108740.

Górny A G, Banaszak Z, Ługowska B, Ratajczak D. 2011. Inheritance of the efficiency of nitrogen uptake and utilization in winter wheat (*Triticum aestivum* L.) under diverse nutrition levels. *Euphytica,* **177**, 191–206.

Guo B, Sleper D A, Lu P, Shannon J G, Nguyen H T, Arelli P R. 2006. QTLs associated with resistance to soybean cyst nematode in soybean meta-analysis of QTL locations — Retraction. *Crop Science*, **46**, 595–602.

Guo Y, Kong F M, Xu Y F, Zhao Y, Liang X, Wang Y Y, An D G, Li S S. 2012. QTL mapping for seedling traits in wheat grown under varying concentrations of N, P and K nutrients. *Theoretical and Applied Genetics,* **124**, 851–865.

Guo Y, Sun J, Zhang G, Wang Y, Kong F, Zhao Y, Li S. 2013. Haplotype, molecular marker and phenotype effects associated with mineral nutrient and grain size traits of *TaGS1a* in wheat. *Field Crops Research*, **154**, 119–125.

Guttieri M J, Frels K, Regassa T, Waters B M, Baenziger P S. 2017. Variation for nitrogen use efficiency traits in current and historical great plains hard winter wheat. *Euphytica*, **213**, 87.

Han X, Zhang M, Gao M, Yuan Y, Yuan Y, Zhang G, An Y, Guo Y, Kong F, Li S. 2023. QTL mapping and candidate gene identifying for N, P, and K use efficiency at the maturity stages in wheat. *Genes*, **14**, 1168.

Hao T, Zhu Q, Zeng M, Shen J, Shi X, Liu X, Zhang F, de Vries W. 2020. Impacts of nitrogen fertilizer type and application rate on soil acidification rate under a wheat–maize double cropping system. *Journal of Environmental Management*, **270**, 110888.

Hao Y C, Kong F M, Wang L L, Zhao Y, Li M Y, Che N X, Li S, Wang M, Hao M, Zhang X C, Zhao Y. 2024. Genome-wide association study of grain micronutrient concentrations in bread wheat. *Journal of Integrative Agriculture*, **23**, 1468–1480.

Hawkesford M J. 2017. Genetic variation in traits for nitrogen use efficiency in wheat. *Journal of Experimental Botany*, **68**, 2627–2632.

He W S. 2003. Genotypic differences in phosphorus utilization efficiency among spring wheat varieties in Ningxia. *Agricultural Research in the Arid Areas*, **2**, 1–6. (in Chinese)

Huang J F, Li L, Mao X G, Wang J Y, Liu H M, Li C N, Jing R L. 2020. dCAPS markers developed for nitrate transporter genes TaNRT2L12s associating with 1 000-grain weight in wheat. *Journal of Integrative Agriculture,* **19**, 1543–1553.

Jing F, Miao Y, Zhang P, Chen T, Liu Y, Ma J, Li M, Yang D. 2022. Characterization of *TaSPP-5A* gene associated with sucrose content in wheat (*Triticum aestivum* L.). *BMC Plant Biology*, **22**, 58.

Kolodziej M C, Singla J, Sánchez-Martín J, Zbinden H, Šimková H, Karafiátová M, Doležel J, Gronnier J, Poretti M, Glauser G, Zhu W, Köster P, Zipfel C, Wicker T, Krattinger S G, Keller B. 2021. A membrane-bound ankyrin repeat protein confers race-specific leaf rust disease resistance in wheat. *Nature Communications,* **12**, 956.

Kreutz G F, Bhadha J H, Sandoya G V. 2022. Examining phosphorus use efficiency across different lettuce (*Lactuca sativa* L.) accessions. *Euphytica*, **218**, 28.

Kusin F M, Akhir N I M, Mohamat-Yusuff F, Awang M. 2015. The impact of nitrogen fertilizer use on greenhouse gas emissions in an oil palm plantation associated with land use change. *Atmosfera*, **28**, 243–250.

Leip A, Ledgard S F, Uwizeye A, Fusi A, Raffa D W. 2018. Nutrient Flows and associated environmental impacts in livestock supply chains. Guidelines for assessment. version 1. FAO, Food and Agriculture Organization of the United Nations, Rome.

Li M X, Yeung J M, Cherny S S, Sham P C. 2012. Evaluating the effective numbers of independent tests and significant *P*-value thresholds in commercial genotyping arrays and public imputation reference datasets. *Human Genetics*, **131**, 747–756.

Li Q, Wang J Y, Khan N, Chang X P, Liu H M, Jing R L. 2016. Polymorphism and association analysis of a drought-resistant gene *TaLTP-s* in wheat. *Journal of Integrative Agriculture*, **15**, 1198–1206.

Li X, Zhang J B, Song B, Li H P, Xu H Q, Qu B, Dang F J, Liao Y C. 2010. Resistance to Fusarium head blight and seedling blight in wheat is associated with activation of a cytochrome P450 gene. *Phytopathology*, **100**, 183–191.

Liang Z, Bronson K F, Thorp K R, Mon J, Badaruddin M, Wang G. 2014. Cultivar and N fertilizer rate affect yield and N use efficiency in irrigated durum wheat. *Crop Science*, **54**, 1175–1183.

Lin Y, Chen G, Hu H, Yang X, Zhang Z, Jiang X, Wu F, Shi H, Wang Q, Zhou K, Li C, Ma J, Zheng Y, Wei Y, Liu Y. 2020. Phenotypic and genetic variation in phosphorus-deficiency-tolerance traits in Chinese wheat landraces. *BMC Plant Biology*, **20**, 330.

Liu H, Wang J, Zhang B, Yang X, Hammond J P, Ding G, Wang S, Cai H, Wang C, Xu F, Shi L. 2021. Genome-wide association study dissects the genetic control of plant height and branch number in response to low-phosphorus stress in *Brassica napus*. *Annals of Botany*, **128**, 919–930.

Liu Q, Zhao Y, Rahman S, She M, Zhang J, Yang R, Islam S, O'Hara G, Varshney R K, Liu H, Ma H, Ma W. 2023. The putative vacuolar processing enzyme gene *TaVPE3cB* is a candidate gene for wheat stem pith-thickness. *Theoretical and Applied Genetics*, **136**, 138.

Ma Z, He S, Wang X, Sun J, Zhang Y, Zhang G, Wu L, Li Z, Liu Z, Sun G, Yan Y, Jia Y, Yang J, Pan Z, Gu Q, Li X, Sun Z, Dai P, Liu Z, Gong W, *et al*. 2018. Resequencing a core collection of upland cotton identifies genomic variation and loci influencing fiber quality and yield. *Nature Genetics*, **50**, 803–813.

Manske G G B, Ortiz-Monasterio J I, van Ginkel M, González R M, Fischer R A, Rajaram S, Vlek P L G. 2001. Importance of P uptake efficiency versus P utilization for wheat yield in acid and calcareous soils in Mexico. *European Journal of Agronomy*, **14**, 261–274.

McDonald G K, Taylor J D, Gong X, Bovill W. 2018. Responses to phosphorus among barley genotypes. *Crop & Pasture Science*, **69**, 574–586.

Meier S, Morales A, López-Olivari R, Matus I, Aponte H, Campos P de S, Khan N, Cartes P, Meriño-Gergichevich C, Castillo D, Seguel A. 2022. Synergistic role between phosphorus and water use efficiency in spring wheat genotypes. *Agricultural Water Management*, **263**, 107481.

Mizutani M, Sato F. 2011. Unusual P450 reactions in plant secondary metabolism. *Archives of Biochemistry and Biophysics*, **507**, 194–203.

Mueth N A, Hulbert S H. 2022. Small RNAs target native and cross-kingdom transcripts on both sides of the wheat stripe rust interaction. *Genomics*, **114**, 110526.

Neff M M, Turk E, Kalishman M. 2002. Web-based primer design for single nucleotide polymorphism analysis. *Trends in Genetics*, **18**, 613–615.

Ober C, Butte A J, Elias J A, Lusis A J, Gan W, Banks-Schlegel S, Schwartz D. 2010. Getting from genes to function in lung disease: A National Heart, Lung, and Blood Institute workshop report. *American Journal of Respiratory and Critical Care Medicine*, **182**, 732–737.

de Oliveira Silva A, Ciampitti I A, Slafer G A, Lollato R P. 2020. Nitrogen utilization efficiency in wheat: A global perspective. *European Journal of Agronomy*, **114**, 126008.

Patial N. 2021. Genetic variability studies in germplasm of wheat (*Triticum aestivum* L.). *Annals of Plant and Soil Research*, **23**, 310–313.

Peng J, Richards D E, Hartley N M, Murphy G P, Devos K M, Flintham J E, Beales J, Fish L J, Worland A J, Pelica F, Sudhakar D, Christou P, Snape J W, Gale M D, Harberd N P. 1999. 'Green revolution' genes encode mutant gibberellin response modulators. *Nature*, **400**, 256–261.

Pinot F, Alayrac C, Mioskowski C, Durst F, Salaun J P. 1994. New cytochrome P450-dependent reactions from wheat: Terminal and sub-terminal hydroxylation of oleic acid by microsomes from naphthalic acid anhydride and phenobarbital induced wheat seedlings. *Biochemical and Biophysical Research Communications*,

198, 795–803.
Quraishi U M, Abrouk M, Murat F, Pont C, Foucrier S, Desmaizieres G, Confolent C, Riviere N, Charmet G, Paux E, Murigneux A, Guerreiro L, Lafarge S, Le Gouis J, Feuillet C, Salse J. 2011. Cross-genome map based dissection of a nitrogen use efficiency ortho-metaQTL in bread wheat unravels concerted cereal genome evolution. *Plant Journal*, **65**, 745–756.
Rengel Z, Damon P M. 2008. Crops and genotypes differ in efficiency of potassium uptake and use. *Physiologia Plantarum*, **133**, 624–636.
Safdar L B, Andleeb T, Latif S, Umer M J, Tang M, Li X, Liu S, Quraishi U M. 2020. Genome-wide association study and QTL meta-analysis identified novel genomic loci controlling potassium use efficiency and agronomic traits in bread wheat. *Frontiers in Plant Science*, **11**, 70.
Safdar L B, Umer M J, Almas F, Uddin S, Safdar Q T, Blighe K, Quraishi U M. 2021. Identification of genetic factors controlling phosphorus utilization efficiency in wheat by genome-wide association study with principal component analysis. *Gene*, **768**, 145301.
Said J I, Lin Z, Zhang X, Song M, Zhang J. 2013. A comprehensive meta QTL analysis for fiber quality, yield, yield related and morphological traits, drought tolerance, and disease resistance in tetraploid cotton. *BMC Genomics*, **14**, 776.
Saini D K, Chopra Y, Pal N, Chahal A, Srivastava P, Gupta P K. 2021. Meta-QTLs, ortho-MQTLs and candidate genes for nitrogen use efficiency and root system architecture in bread wheat (*Triticum aestivum* L.). *Physiology and Molecular Biology of Plants*, **27**, 2245–2267.
Shi H, Chen M, Gao L, Wang Y, Bai Y, Yan H, Xu C, Zhou Y, Xu Z, Chen J, Tang W, Wang S, Shi Y, Wu Y, Sun D, Jia J, Ma Y. 2022. Genome-wide association study of agronomic traits related to nitrogen use efficiency in wheat. *Theoretical and Applied Genetics*, **135**, 4289–4302.
Shi H, Wang W, Gao L, Wu J, Hu C, Yan H, Shi Y, Li N, Ma Y, Zhou Y, Xu Z, Chen J, Tang W, Chen K, Sun D, Wu Y, Chen M. 2023. Genome-wide association study of seedling nitrogen-use efficiency-associated traits in common wheat (*Triticum aestivum* L.). *The Crop Journal*, **12**, 222–231.
Sosnowski O, Charcosset A, Joets J. 2012. BioMercator V3: An upgrade of genetic map compilation and quantitative trait loci meta-analysis algorithms. *Bioinformatics*, **28**, 2082–2083.
Soumya P R, Burridge A J, Singh N, Batra R, Pandey R, Kalia S, Rai V, Edwards K J. 2021. Population structure and genome-wide association studies in bread wheat for phosphorus efficiency traits using 35 K Wheat Breeder's Affymetrix array. *Scientific Reports*, **11**, 7601.
Su J Y, Zheng Q, Li H W, Li B, Jing R L, Tong Y P, Li Z S. 2009. Detection of QTLs for phosphorus use efficiency in relation to agronomic performance of wheat grown under phosphorus sufficient and limited conditions. *Plant Science*, **176**, 824–836.
Sun C, Dong Z, Zhao L, Ren Y, Zhang N, Chen F. 2020. The Wheat 660K SNP array demonstrates great potential for marker-assisted selection in polyploid wheat. *Plant Biotechnology Journal*, **18**, 1354–1360.
Thiemann A, Fu J, Seifert F, Grant-Downton R T, Schrag T A, Pospisil H, Frisch M, Melchinger A E, Scholten S. 2014. Genome-wide meta-analysis of maize heterosis reveals the potential role of additive gene expression at pericentromeric loci. *BMC Plant Biology*, **14**, 88.
Venske E, Dos Santos R S, Farias D d R, Rother V, da Maia L C, Pegoraro C, Oliveira A C d. 2019. Meta-analysis of the QTLome of Fusarium head blight resistance in bread wheat: Refining the current puzzle. *Frontiers in Plant Science*, **10**, 727.
Veyrieras J B, Goffinet B, Charcosset A. 2007. MetaQTL: A package of new computational methods for the meta-analysis of QTL mapping experiments. *BMC Bioinformatics*, **8**, 49.
Vo K T X, Kim C Y, Chandran A K N, Jung K H, An G, Jeon J S. 2015. Molecular insights into the function of ankyrin proteins in plants. *Journal of Plant Biology*, **58**, 271–284.
Wang L, Liu Y J, Xiao P, Shen H, Deng H Y, Papasian C J, Drees B M, Hamilton J J, Recker R R, Deng H W. 2007. Chromosome 2q32 may harbor a QTL affecting BMD variation at different skeletal sites. *Journal of Bone and Mineral Research*, **22**, 1672–1678.
Xiong R, He T, Wang Y, Liu S, Gao Y, Yan H, Xiang Y. 2021. Genome and transcriptome analysis to understand the role diversification of cytochrome P450 gene under excess nitrogen treatment. *BMC Plant Biology*, **21**, 447.
Xu J, Gao Z, Liu S, Elwafa S F A, Tian H. 2022. A multienvironmental evaluation of the N, P and K use efficiency of a large wheat diversity panel. *Field Crops Research*, **286**, 108634.
Xu Y, Wang R, Tong Y, Zhao H, Xie Q, Liu D, Zhang A, Li B, Xu H, An D. 2014. Mapping QTLs for yield and nitrogen-related traits in wheat: influence of nitrogen and phosphorus fertilization on QTL expression. *Theoretical and Applied Genetics*, **127**, 59–72.
Yan S N, Yu Z Y, Gao W, Wang X Y, Cao J J, Lu J, Ma C X, Chang C, Zhang H P. 2023. Dissecting the genetic basis of grain color and pre-harvest sprouting resistance in common wheat by association analysis. *Journal of Integrative Agriculture*, **22**, 2617–2631.
Yang H, Chen R, Chen Y, Li H, Wei T, Xie W, Fan G. 2022. Agronomic and physiological traits associated with genetic improvement of phosphorus use efficiency of wheat grown in a purple lithomorphic soil. *The Crop Journal*, **10**, 1151–1164.
Yang J, Wang M, Li W, He X, Teng W, Ma W, Zhao X, Hu M, Li H, Zhang Y, Tong Y. 2019. Reducing expression of a nitrate-responsive bZIP transcription factor increases grain yield and N use in wheat. *Plant Biotechnology Journal*, **17**, 1823–1833.
Yang M J, Wang C R, Hassan M A, Wu Y Y, Xia X C, Shi S B, Xiao Y G, He Z H. 2021. QTL mapping of seedling biomass and root traits under different nitrogen conditions in bread wheat (*Triticum aestivum* L.). *Journal of Integrative Agriculture*, **20**, 1180–1192.
Yang S Y, Lin W Y, Hsiao Y M, Chiou T J. 2024. Milestones in understanding transport, sensing, and signaling of the plant nutrient phosphorus. *The Plant Cell*, **36**, 1–20.
Yang Y, Amo A, Wei D, Chai Y, Zheng J, Qiao P, Cui C, Lu S, Chen L, Hu Y G. 2021. Large-scale integration of meta-QTL and genome-wide association study discovers the genomic regions and candidate genes for yield and yield-related traits in bread wheat. *Theoretical and* Applied *Genetics*, **134**, 3083–3109.
Yu S Z, Wu J H, Wang M, Shi W M, Xia G M, Jia J Z, Kang Z S, Han D J. 2020. Haplotype variations in QTL for salt tolerance in Chinese wheat accessions identified by marker-based and pedigree-based kinship analyses. *Crop Journal*, **8**, 1011–1024.
Zhang L, Zhang L, Xia C, Gao L, Hao C, Zhao G, Jia J, Kong X. 2017. A novel wheat C-bZIP gene, *TabZIP14-B*, participates in salt and freezing tolerance in transgenic plants. *Frontiers in Plant Science,* **8**, 710.
Zhang L Y, Liu D C, Guo X L, Yang W L, Sun J Z, Wang D W, Zhang A. 2010. Genomic distribution of quantitative trait loci for yield and yield-related traits in common wheat. *Journal of Integrative Plant Biology*, **52**, 996–1007.
Zhang M, Gao M, Zheng H, Yuan Y, Zhou X, Guo Y, Zhang G, Zhao Y, Kong F, An Y, Li S. 2019. QTL mapping for nitrogen use efficiency and agronomic traits at the seedling and maturity stages in wheat. *Molecular Breeding*, **39**, 71.
Zhang X, Jia H, Li T, Wu J, Nagarajan R, Lei L, Powers C, Kan C C, Hua W, Liu Z, Chen C, Carver B F, Yan L. 2022. *TaCol-B5* modifies spike architecture and enhances grain yield in wheat. *Science*, **376**, 180–183.
Zhang Y, Zhang G, Xia N, Wang X J, Huang L L, Kang Z S. 2008. Cloning and characterization of a bZIP transcription factor gene in wheat and its expression in response to stripe rust pathogen infection and abiotic stresses. *Physiological and Molecular Plant Pathology*, **73**, 88–94.
Zhang Z P, Li Z, He F, Lü J J, Xie B, Yi X Y, Li J M, Li J, Song J H, Pu Z E, Ma J, Peng Y Y, Chen G Y, Wei Y M, Zheng Y I, Li W. 2023. Genome-wide association and linkage mapping strategies reveal the genetic loci and candidate genes of important agronomic traits in Sichuan wheat. *Journal of Integrative Agriculture*, **22**, 3380–3393.
Zhou X, Stephens M. 2012. Genome-wide efficient mixed-model analysis for association studies. *Nature Genetics*, **44**, 821–824.

Executive Editor-in-Chief Xueyong Zhang
Managing Editor Ning Wang